AD-A077 162 MALLORY (P R) AND CO INC BURLINGTON MASS LAB FOR PH--ETC F/G 10/3
LITHIUM-THIONYL CHLORIDE BATTERY. (U)
NOV 79 A N DEY , N HAMILTON , W BOW DEN DAAB07-78-C-0563

UNCLASSIFIED

1 OF 1
AD A077182

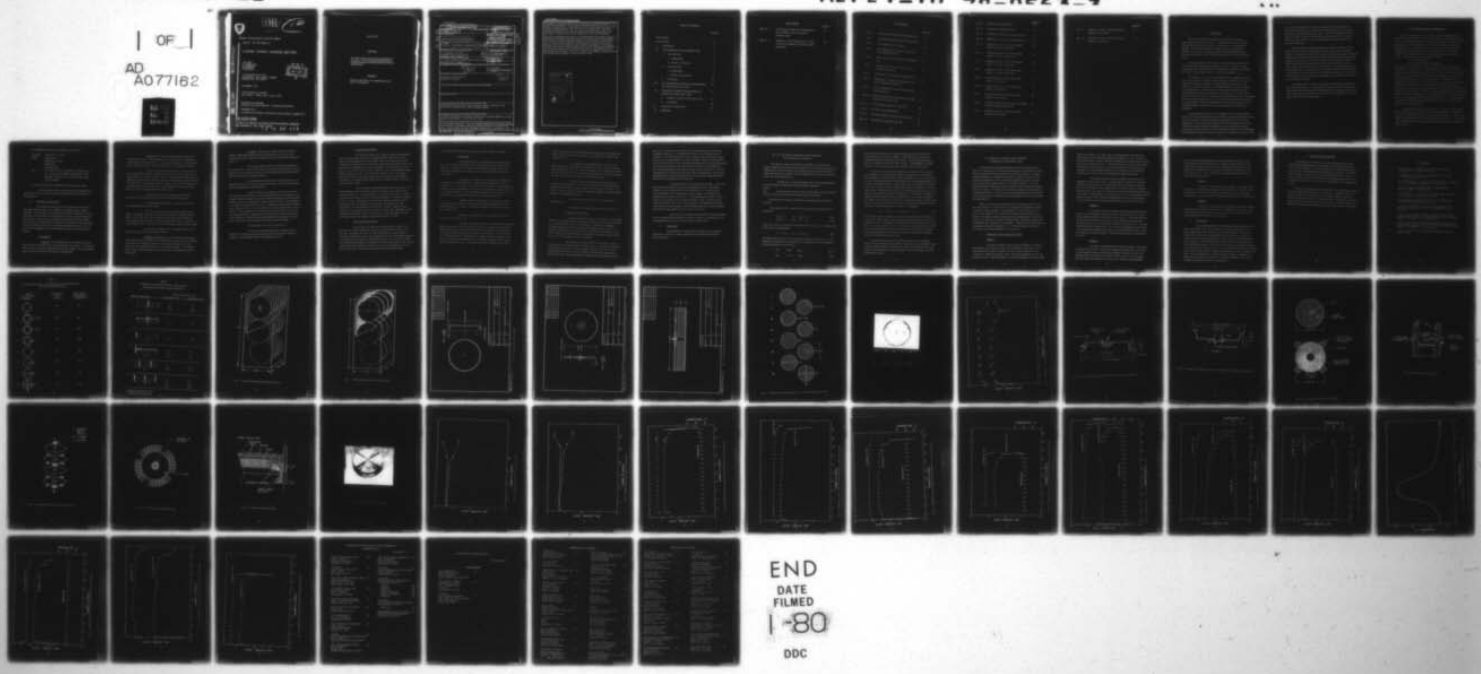

END
DATE FILMED
1-80
DDC

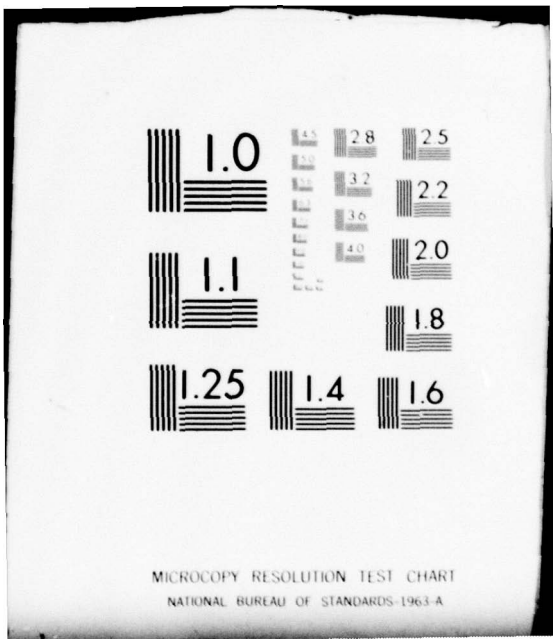
1.0
1.1
1.25
1.4
1.6
1.8
2.0
2.2
2.5
2.8
3.2
3.6
4.0
MICROCOPY RESOLUTION TEST CHART
NATIONAL BUREAU OF STANDARDS-1963-A

LEVEL II

A072358

Research and Development Technical Report

DELET-TR-78-0563-3

LITHIUM-THIONYL CHLORIDE BATTERY

A.N. DEY
N. HAMILTON
W. BOWDEN
P. WITALIS

P.R. MALLORY & CO, INC.
LABORATORY FOR PHYSICAL SCIENCE
BURLINGTON, MA 01803

NOVEMBER 1979

THIRD QUARTERLY REPORT
FOR PERIOD 1 APRIL 1979 - 31 JULY 1979

DISTRIBUTION STATEMENT :
APPROVED FOR PUBLIC RELEASE ; DISTRIBUTION UNLIMITED

PREPARED FOR :
U S ARMY ELECTRONICS TECHNOLOGY AND DEVICES LABORATORY

ERADCOM

US ARMY ELECTRONICS RESEARCH AND DEVELOPMENT COMMAND
FORT MONMOUTH, NEW JERSEY 07703

NOTICES

Disclaimers

The citation of trade names and names of manufacturers in this report is not to be construed as official Government indorsement or approval of commercial products or services referenced herein.

Disposition

Destroy this report when it is no longer needed. Do not return it to the originator.

Unclassified

SECURITY CLASSIFICATION OF THIS PAGE (When Data Entered)

REPORT DOCUMENTATION PAGE	READ INSTRUCTIONS BEFORE COMPLETING FORM
1. REPORT NUMBER: DELET-TR-78-0563-3	2. GOVT ACCESSION NO. / 3. RECIPIENT'S CATALOG NUMBER
4. TITLE (and Subtitle): Lithium-Thionyl Chloride Battery	5. TYPE OF REPORT & PERIOD COVERED: Third Quarterly Report, no. 3, 4/1/79 to 7/31/79
	6. PERFORMING ORG. REPORT NUMBER: 1 apr - 31 jul 79
7. AUTHOR(s): A. N. Dey, N. Hamilton, W. Bowden, P. Witalis	8. CONTRACT OR GRANT NUMBER(s): DAAB07-78-C-0563
9. PERFORMING ORGANIZATION NAME AND ADDRESS: P. R. Mallory & Co. Inc. Laboratory for Physical Science Burlington, Mass. 01803	10. PROGRAM ELEMENT, PROJECT, TASK AREA & WORK UNIT NUMBERS: 1L162705AH94 -219
11. CONTROLLING OFFICE NAME AND ADDRESS: U. S. Army Electronics Technology & Device Lab. ERADCOM Attn: DELET-PR Ft. Monmouth, New Jersey 07703	12. REPORT DATE: November 1979 / 13. NUMBER OF PAGES: 48
14. MONITORING AGENCY NAME & ADDRESS (If different from Controlling Office)	15. SECURITY CLASS. (of this report): Unclassified / 15a. DECLASSIFICATION/DOWNGRADING SCHEDULE

16. DISTRIBUTION STATEMENT (of this Report)

Approved for Public Release
Distribution Unlimited

17. DISTRIBUTION STATEMENT (of the abstract entered in Block 20, if different from Report)

18. SUPPLEMENTARY NOTES

19. KEY WORDS (Continue on reverse side if necessary and identify by block number)

Inorganic electrolyte battery, thionyl chloride, lithium, high rate D cell, high rate flat cylindrical cell, laser designator battery.

20. ABSTRACT (Continue on reverse side if necessary and identify by block number)

This report summarizes the activities carried out on Contract DAAB07-78-C-0563 during the period April 1, 1979 to July 31, 1979.

We have designed and built three inch diameter $Li/SOCl_2$ flat cells for the GLLD laser designator application. This cell showed exceedingly low internal impedance and maintained an operating voltage above three volts on 17.5A pulse for 26 bursts. The presently used Ni/Cd batteries deliver only 3 such bursts. The

DD FORM 1 JAN 73 1473 EDITION OF 1 NOV 65 IS OBSOLETE

215 325

Unclassified

SECURITY CLASSIFICATION OF THIS PAGE (When Data Entered)

exceedingly low cell polarization on load resulted in negligible temperature rise during the cell operation. The maximum cell temperature was below 29°C. The cell was designed with a low pressure vent which opened during cell abuse by extended forced-discharge. The cell met all our design goals. We plan to continue to optimize the cell design and the cell fabrication procedures for improving the safety and the efficient fabrication of the cell respectively.

The cyclic voltammetric work carried out during the first two quarters for elucidating the cell reaction mechanism paid off handsomely in terms of providing a new approach to improve both the performance and the safety of the $Li/SOCl_2$ cells. We evaluated the efficacy of the approach using the ultra-high rate spirally wound D cells developed during the first two quarters. We developed two types of catalytic cathode additives which promote the chemical reactions of the unstable species to form stable products thus contributing to both the performance and the safety. We plan to optimize this approach further during the next quarter and incorporate this in flat cells as well.

TABLE OF CONTENTS

		Page No.
List of Tables		i
List of Figures		ii
I.	Introduction	1
II.	The Development of Flat Cylindrical Cell	3
	A. Thin Flat Cell	4
	1. Experimental	4
	2. Results & Discussion	7
	B. Thick Flat Cell	7
	1. Experimental	8
	2. Results and Discussion	9
	C. Conclusions	10
III.	The Cell Reaction Mechanism and Its Implication On Cell Performance and Safety	11
IV.	Evaluation of Catalytic Cathode Additives in Spirally Wound High Rate D Cells	13
	A. Testing of D Cells on GLLD Duty Cycle	13
	B. Conclusions	15
V.	Conclusions & Future Work	16
VI.	References	17

List of Tables

		Page No.
Table No. 1	Short-Circuit Currents of the Experimental Flat Cylindrical Cells with Various Cathode Designs	18
Table No. 2	Performance of High Rate Li/$SOCl_2$ D Cells on GLLD and Modified GLLD Tests at Room Temperature	19

List of Figures

		Page No.
Fig. 1	Laser designator battery with thin flat cells	20
Fig. 2	Laser designator battery with thick flat cells	21
Fig. 3	Flat cylindrical cell container	22
Fig. 4	Flat cylindrical cell top with G/M seal and the electrolyte fill port	23
Fig. 5	Cross-Section of the hermetic flat cylindrical cell	24
Fig. 6	Current collector designs for the 2.8 inch diameter disc cathodes	25
Fig. 7	Photograph of a hermetic flat cylindrical cell	26
Fig. 8	Performance of hermetic flat cylindrical cell with 8 cathodes on GLLD test	27
Fig. 9	Top of hermetically sealed flat cell with G/M seal and fill tube	28
Fig. 10	Bottom of hermetically sealed flat cell showing low pressure G/M seal vent	29
Fig. 11	The anode and cathode for a flat cell	30
Fig. 12	The flat cell assembly fixture	31
Fig. 13	Assembly stacking sequence for the flat cell	32
Fig. 14	Top view of an assembled flat cell	33

		Page No.
Fig. 15	Lithium anode contact detail	34
Fig. 16	Photograph of finished flat cell	35
Fig. 17	Performance of flat cell on GLLD test cycle	36
Fig. 18	Performance of flat cell on GLLD test cycle	37
Fig. 19	Performance of two D cells with cathode additive, level A on GLLD test	38
Fig. 20	Performance of two D cells with cathode additive 1, level A on GLLD test	39
Fig. 21	Performance of two D cells with cathode additive 1, level B on GLLD test	40
Fig. 22	Performance of two D cells with cathode additive 1, level B on GLLD test.	41
Fig. 23.	Performance of two D cells with cathode additive 2 on GLLD test	42
Fig. 24	Performance of two D cells with cathode additive 2 on GLLD test	43
Fig. 25	Performance of two D cells with cathode additive 3 on GLLD test	44
Fig. 26	Cell wall temperature of 2 D cells with cathode additive 3 during reversal at 2A.	45
Fig. 27	Performance of two D cells with cathode additive 3 on GLLD test	46

		Page No.
Fig. 28	Performance of two D cells with cathode additive 4 on GLLD test	47
Fig. 29	Performance of two D cells with cathode additive 5 on GLLD test	48

I. Introduction

The $Li/SOCl_2$ inorganic electrolyte system (1-4) is the highest energy density system known to date. It consists of a Li anode, a carbon cathode and $SOCl_2$ which acts both as a solvent and as a cathode active material. The electrolyte salt that has been used most extensively is $LiAlCl_4$, but salts such as $Li_2B_{10}Cl_{10}$ (5) and $Li_2C(AlCl_3)_2$ (6) have also been used successfully in this system for improving the shelf life characteristics.

The main objective of this program is to develop high rate $Li/SOCl_2$ cells and batteries for portable applications of the U. S. Army. The cells and batteries must deliver high energy densities than are presently available and must be safe to handle under U. S. Army field conditions.

We carried out a detailed development (7) on the spirally-wound high rate D cells in order to establish their performance capabilities as well as to identify and correct the limitations in their performance and safety under various use and abuse conditions. Substantial progress was made to correct the cell limitations. We found that the state-of-the-art spirally-wound D cells approach the high rate requirements of the various U. S. Army applications more closely than do any other cell designs at the present time. Accordingly we have used this spirally-wound D cell as a starting point and have improved its rate capability to meet the requirements of two specific applications, viz. the BA5590 Battery for Man Pack Radio and the Battery for the GLLD Laser Designator.

We concentrated our effort on the development of the spirally-wound ultra-high rate D cell during the first two quarters, in order to determine whether it will be possible to meet the performance requirements of the GLLD laser designators. The results obtained during the second quarter indicate that the high rate D cells are capable of delivering as high as eighteen (18) bursts compared to the three (3) bursts realized from the presently used Ni/Cd batteries. The advantage of using the D cells, as opposed to a flat cell, is that the D cells

can be readily manufactured at our lithium battery manufacturing plant with very slight modification of the existing manufacturing process used for manufacturing the spirally wound Li/SO_2 D cells. The results obtained to date are highly encouraging and we are continuing to improve the $Li/SOCl_2$ D cells so that it can meet a variety of high rate requirements including the GLLD laser designator application.

During the third quarter we primarily concentrated our effort on the development of the three inch diameter flat cell for the GLLD Laser Designator Battery. We initiated the procurement of parts during the first quarter. The detail designing of the flat cell and the parts and the design and fabrication of tooling needed to make the parts and the cell have been mostly completed during the third quarter. We have developed two types of flat cell structures; one is 0.45 inch thick and the other one is 0.90 inch thick. The packaging efficiency of the battery with 0.9 inch thick cell is significantly higher than that with the 0.45 inch thick cell since it requires 8 cells/battery instead of 16 cells/battery. The construction and the performance characteristics of both types of flat cells are described in this report.

During the first two quarters we examined the cell reaction mechanisms using cyclic voltammetry. The information obtained from this study indicated several approaches for improving the performance and the safety of the $Li/SOCl_2$ cells. We evaluated the efficacy of these approaches in spirally wound D cells. These will be discussed in this report.

II. The Development of Flat Cylindrical Cell

The high surface area to volume ratio of the flat cylindrical cell enhances the heat dissipation of the cell from its surface to the environment and as such is a better configuration from the safety standpoint. However, this is true in the case of single cells only. In the case of multicell battery, the individual cells may be potted in such a manner that they may be thermally insulated from the environment and the heat dissipation may be rather insignificant. Therefore, reliance on heat dissipation of cells for safety is unsound. For this reason, we have attempted to achieve,

(a) low heat generation

(b) high internal thermal equilibration

in the design of our flat cells. In this manner, the cells will be safe when used either as single cells or as multicell batteries. The design objective is to balance the total heat generation during the high current pulses with the total thermal mass of the battery such that the internal temperature of the cells does not exceed the upper limit of the safe temperature. We determined this temperature (7) by doing DTA of the cell constituents and found that the lowest temperature of initiation of an exothermic reaction is 150° C for the Li + S combination. S is a reaction product of the cell. This exothermic reaction may initiate a thermal runaway. Therefore, the internal temperature of the cell should be kept below that. Arbitrarily, we chose an upper limit of the safe temperature of 130° C. In addition, we developed a safety vent for these flat cells so that on accidental short circuiting or force-discharge, the cells will vent prior to reaching the above temperatures.

We have developed two types of flat cells, both are 3 inch in diameter. One is 0.45 inch thick. Sixteen of these cells, connected two in parallel and 8 in series, are required for one GLLD laser designator battery. A sketch of the battery pack with sixteen 0.45 inch flat cells is shown in Fig. 1. The other flat cell is approximately 0.90 inch thick and it requires eight cells per battery as shown in Fig. 2.

The specifications for the above battery are as follows:

Dimension:	2.82" x 3.75" x 9.30"
Voltage:	Nominal 24V
	Maximum (OCV) 32V
	Average 24V
	End Voltage 20V
Duty:	17.5A for 35.5 m.sec. followed by 1.8A for 14.5 m. sec. and the cycle continues for 3 minutes. This constitutes one burst. This 3 minute cycle occurs every 30 minutes.

The presently used Ni/Cd batteries provide 3 bursts per charge.

The details of the design, construction and the performance of the two types of flat cells that we have developed for the above battery are described here.

A. Thin Flat Cell (0.45 inch)

We initiated the design and the procurement of parts for this cell during the first quarter and completed a substantial portion of these activities. All the tooling, jigs and fixtures required to fabricate the various cell parts and to assemble the electrode stack has been completed during the third quarter. In view of the encouraging results obtained from the spirally wound D cells, we temporarily discontinued the development of this cell during the second quarter in favor of the continuing improvement of the D cell. We refocussed our attention on the development of the flat cell during the third quarter.

1. Experimental

Cell Can: The specifications of the stainless steel can which is 3 inch in diameter and 0.45 inch high are shown in Fig. 3. The procurement of this can has been completed during the first quarter. The cans received from the vendor were found to be within the specification.

Cell Top: The design of the cover of the cell is shown schematically in Fig. 4. The stainless steel cover which has an interference fit with the cell can shown in Fig. 3, was also procured from an outside vendor and the parts were found to be acceptable based on the tolerances specified.

The glass-to-metal seal loacted on the cell top consists of an outer metallic rang and a central post both of which were custom made by outside vendors. The glass preforms were also procured from outside vendor. A graphite boat with multiple cavity was designed and fabricated to make the glass-to-metal seals. A multi-zoned quartz tube furnace was used for the firing and annealing of the glass-to-metal seals. The optimization of the seal making process has been completed during the third quarter.

A punching tool has been designed and fabricated to punch out holes on the cover for the seal and the electrolyte fill port.

The electrolyte fill port tube, as shown in Fig. 4, was also procured from an outside vendor.

The glass-to-metal seal was resistance welded to the cover. The welding step was found to be quite critical in obtaining hermetic welds. The design of the metal seal body, the location and the contour of the projection on the seal body, all played an important role in accomplishing rugged hermetic welds. The process has been developed during the third quarter.

The resistance welding of the electrolyte fill tube to the cell top was found to be fairly straight forward.

Welding of Cell Top to Can: We designed and fabricated elaborate heat sinking fixtures for TIG welding the top to the can. The elaborate heat-sinking was needed to prevent excessive internal heating of the cell which may have undesirable effects on the electrode materials. The welding process was developed during the first quarter but it was perfected during the third quarter.

The Cell: Circular donut shaped anodes and cathodes and glass filter paper separators were used to make this cell. The cross-sectional view of the cell and the electrode stack is schematically represented in Fig. 5.

The current collector design chosen for the cathode was #6 shown in Fig. 6. This had the highest short circuit current density of all the designs (as shown in Table 3) based on the results from the demountable cells discussed in the first quarterly report (8).

The electrical conductivity of the lithium anode was sufficiently high so that no current collector was needed. Disc shaped Li anodes were welded directly to the feed through.

The glass filter paper separators used to make the cell was found to be rather fragile. The successful assembly of the electrode stack required extensive fixturing and special handling procedures to prevent internal shorting. The cell contained eight cathodes and nine anodes. The diameter of the cathode was approximately 2.8 inch. Therefore, the total effective cathode area, using both sides, was approximately 70 cm^2/per cathode with a total of 560 cm^2. This corresponds to a current density of 31 mA/cm^2 on 17.5 A load. The carbon cathode was approximately 0.015 inch thick and the Li anode was 0.010 inch thick. The glass filter paper separator was nominally 0.005 inch thick. Two layers of the separators were used to prevent shorting.

The photograph of a cell is shown in Fig. 7.

The cell was evacuated through the fill port and then filled with 1.8M $LiAlCl_4$-$SOCl_2$ electrolyte and the fill port was closed by welding. The electrolyte weight was approximately 44 gms.

2. Results and Discussion

The cell was tested at 25°C under the GLLD laser designator duty cycle involving 17.5A pulse as described earlier. Although, two cells will be used in parallel in the actual battery and as such the single cell will experience only half the load, we tested the single cell on the full load of 17.5A because of the inflexibility of the test equipment. The cell voltage on the two loads, viz 17.5A for 35.5 m.sec and 1.8A for 14.5 m.sec were monitored during the three minute duty cycle. The results are shown in Fig. 8. The voltage profiles are shown for each three minute bursts and the results are plotted as a function of the number of bursts instead of as a function of time. Each burst occurs every 27 minutes.

The cell showed some voltage-delay on the first cycle. The cell polarization on 17.5A load was found to be rather severe, although the operating voltage at 17.5A remained above 2.5 volt most of the time. In order to meet the end voltage of 20 volt for the whole battery, the single cell voltage must be 2.5 volt. Considering the fact that the cell was subjected to twice the required load, the operating cell voltage was considered to be quite satisfactory. The cell delivered 8 bursts above 2.0 volt. With two cells in parallel, one may expect at least 16 bursts or possibly more. With two D Cells in parallel, we realized about 17 bursts above 2.5 volt. Therefore, this flat cell did not provide any significant improvement over the D cells.

B. Thick Flat Cell (0.90 inch)

In this design, the flat cell is not only twice as thick as the previous one, but the welding lip is located halfway between the two faces of the cell. Essentially, the cell can comes in two halves of equal thickness. The volume not utilized by the active ingredients because of the welding projection is significantly less than that in the previous design. Also, the space wasted due to intercell connections is minimized by reducing the number of cells, although the thickness of the stainless steel wall of the can was increased from 0.019 inch to 0.032 inch in this design in order to make the cell more rugged

and capable of withstanding high pressures without bulging or rupturing.

1. Experimental

A substantial fraction of our effort during the third quarter has been directed to developing methods for fabrication and assembly of this flat cell. In contrast to our relatively well developed spirally wound cell technology, there were many problem areas in which difficulties have had to be overcome.

Cell Can: The flat cell can is of two piece construction, consisting of a cell top and bottom. Both parts are constructed of 0.032" stainless steel. The details of the cell top is shown in Fig. 9. It incorporates a fill tube which is internally welded and a G/M seal which is joined to the top by resistance welding. The cell can bottom details are shown in Fig. 10. It incorporates the low pressure vent which is TIG welded to the can.

Cathode: The flat cell cathode is made up of a carbon-PTFE blend (90-10%) which is pasted on an expanded metal grid, rolled to the desired thickness and cured. The cathodes are then cut to shape as shown in Fig. 11 with a die.

Anode: The flat cell anode is a circular disc of 0.005" Li foil, cut to size with a die.

The Cell: The electrode stack is assembled in a five pronged fixture shown in Fig. 12 which indexes the anode, cathode and separator with proper offset for the cathode current collector. The assembly order incorporates an expanded metal washer above and below each anode disc, as shown in Fig. 13. The electrode stack is terminated by a double anode and separator at each end to give better heat transmission. The assembled electrode stack is tested for short circuits to the can. A hollow threaded bolt is inserted on the center

of the stack and a nut is screwed down of the exmet washers to assure good anode contact. The finished cell stack has an appearance similar to that shown in Fig. 14.

The hollow bolt is then topped with a plug of Li and pressed onto the anode center post, extruding the Li plug to give a positive anode contact (Fig. 15). The cell top and bottom are now fitted together with the ends of the cathode current collector tabs protruding. The tabs are trimmed with scissors and the cell is closed by TIG welding the rim.

The cell is tested for internal short circuits using an ohmmeter and evacuated to 0.2 mm Hg. The cell is then filled with 1.8M $LiAlCl_4/SCCl_2$ electrolyte using vacuum in the cell to provide suction. The cell resistance is monitored during evacuation and voltage is monitored during filling as a precautionary measure.

The cells were tested on GLLD laser designator duty cycle at 25°C.

A photograph of the finished cell is shown in Fig. 16.

2. Results and Discussion

One cell contained 40 cathodes and 41 anodes. The electrode stack was subjected to extensive compressive force and mechanical shock after the assembly in order to check the integrity of the separator. Improperly assembled electrode stack will show internal shorting under such tests. The electrode stacks which survive such high compressive and mechanical shocks were selected for the final welding and filling with electrolyte. This cell contained 75 gm of 1.8M $LiAlCl_4$-$SCCl_2$ electrolyte.

The voltage of the cell on both the 17.5A load and on the 1.8A load (as per the duty cycle) are shown in Fig. 17. Note that on increasing the load from 1.8A to 17.5A, the cell voltagd drops from 3.4V to 3.35 volt, a polarization of only 50 mV. This is a major accomplishment in the design of the high rate cell. This demonstrates the efficacy of the electrode designs in

terms of the current collector design and the electrode separation on the rate capability of the cells. Cells delivered 18 bursts, at which point the cell voltage on 17.5A was still above 3.0 volt. The cell was shut off at this stage because of the malfunctioning of our test equipment. Later on, the vend lid of the cell fell off because of the mishandling resulting from an unrelated experiment that was going on nearby. In spite of this, the result was very impressive. The maximum temperature of the cell was found to be less than 29° C. This low temperature rise is expected in view of the low cell polarization. The low heat generation during the high current pulse is one of our major design objectives that we have accomplished by this flat cell.

Another flat cell had 35 cathodes and 36 anodes. This cell was also tested under the GLLD laser designator duty cycle. The voltage profiles on the three minute bursts are shown in Fig. 18. Exceedingly low cell polarization on high current pulse is again noted. The maximum cell temperature was again less than 29° C. The cell delivered 26 bursts at which point, the cell voltage on 17.5A pulse was still 3.0 volt. The cell was automatically shut off at this stage. This represents a 44% improvement in terms of the number of bursts obtained over that obtained from two D cells in parallel. The capacity corresponding to the 26 bursts is 16.9 A.Hr.

The cell was abused after the above test by force-discharging at 2A. The cell delivered another 2.2 A.Hr to 2.0 volt. On cell reversal, the cell temperature rose to 49° C at which point the cell vented.

C. Conclusions

The performance of the thick flat cell met most of our design objectives. We plan to continue optimizing the cell further for increased abuse resistance.

III. The Cell Reaction Mechanism and Its Implication On Cell Performance and Safety

We carried out cyclic voltammetric, coulometric and spectroscopic studies during the first and the second quarters (9) in an effort to gain increased understanding of the cell reaction mechanisms with the hope that this will be useful in finding ways to improve both the performance and the abuse resistance of the cell. We discovered that

(a) there was an apparent depletion and subsequent regeneration of $SOCl_2$ during the potentiostatic electrochemical reduction of $SOCl_2$,

and (b) the absence of both S and SO_2 immediately after the reduction of $SOCl_2$; and these are generated gradually after the reduction.

We proposed the following cell reaction mechanism in order to explain the above.

The reduction of $SOCl_2$ involves two successive one electron steps to generate SO,

$$SOCl_2 + e \longrightarrow SOCl + Cl^- \qquad [1]$$

$$SOCl + e \longrightarrow SO + Cl^- \qquad [2]$$

At the early stages of discharge, in presence of excess $SOCl_2$, SO combines with $SOCl_2$ to form an intermediate

$$SO + SOCl_2 \longrightarrow SO \cdot SOCl_2 \qquad [3]$$

The intermediate species $SO \cdot SOCl_2$ slowly decomposes to form $SOCl_2$. As the electrolysis progresses the concentration of SO increases and the dimerization and polymerization of SO is favored.

$$2SO \longrightarrow (SO)_2 \qquad [4]$$

$$nSO \longrightarrow (SO)_n \qquad [5]$$

We had some spectroscopic and cyclic voltammetric evidence (9) in favor of the formation of the dimer or polymer. These dimers and polymers are kinetically stable and decompose to S and SO_2. The decomposition process may be accelerated by heat or by other catalysts. Under suitable conditions formation of solid stable sulfur-oxygen polymers may also be possible.

Based on the above reaction mechanism it occurred to us that a lot of the instability and sudden pressure build-up and explosions associated with the discharged and force-discharge $Li/SOCl_2$ batteries may be due to the formation of the kinetically stable but thermodynamically unstable intermediates such as $(SO)_n$. The decomposition of $(SO)_n$ to form SO_2 may be triggered by various means such as shock, or local heating during a force-discharge, etc. and this could lead to a rapid pressure build-up. This decomposition process may also produce sufficient heat to trigger the explosive Li + S reaction. Therefore, one approach towards improved safety involves the use of a catalytic material in the carbon cathode which will catalyze the decomposition of the unstable species such as $(SO)_n$ so that during cell discharge, the cell reaction will result in the formation of stable reaction products S and SO_2 according to

$$4\ Li + 2SOCl_2 \longrightarrow 4\ LiCl + S + SO_2 \qquad [6]$$

In this manner the pressure build-up and the heat evolution (if any) during the cell discharge will be gradual and predictable instead of being sudden and unpredictable. Also, the addition of catalyst may prevent the formation of species such as $SO \cdot SOCl_2$, and thus increase the efficiency of $SOCl_2$ reduction at high rates. The formation of $SO \cdot SOCl_2$ does not affect the efficiency at low rates as demonstrated earlier (10) where we discharged $SOCl_2$ with 98% efficiency based on 2 electrons per mole of $SOCl_2$.

We evaluated the efficacy of the above approach by incorporating various catalytic additives in the carbon cathode of the high rate spirally wound D cells and testing their performance on the GLLD laser designator duty cycle and their abuse resistance on force-discharge. This is described in the next section of this report.

IV. Evaluation of Catalytic Cathode Additives In Spirally Wound High Rate D Cells

We found that the current distribution in high rate spirally wound D cells was controlled by the electrical conductivity of the cathode grid in cells with one current collector tab located at an end of the cathode. To control current distribution, we examined the effect of a variety of cathode current collector configurations on the short circuit current density at the cathode. These results from the first quarter are summarized in Table 1. The most promising cathode configurations were evaluated using the GLLD and modified GLLD duty cycles. Our results with the high rate electrode configurations are summarized in Table 2. In these tests a great improvement was demonstrated by the change from the conventional cell configuration C to the end and central tab configuration F.

Since we have now an optimized cathode configuration (F) for use in the GLLD battery, we used these types of cathodes for evaluating the efficacy of catalytic cathode additives on the performance and abuse resistance of cells. These additives were selected from materials which are known to be catalysts for various chemical reactions and are compatible with the $Li/SOCl_2$ system. We selected six catalytic additives after a preliminary screening for compatibility with electrolyte and availability. Additive 1 was evaluated at two composition levels while additives 2, 3, 4, 5 have only been evaluated at one level using cathode configuration F in all cases.

A. Testing of D Cells on GLLD Duty Cycle

Additive 1

Two pairs of spirally wound D cells with additive 1 at level A were tested on the GLLD duty cycle. In the first pair of cells (Fig. 19) the load voltage for the first 17.5A pulse was 2.6V, with an increase to 2.9V through the 3 minute pulse regime. The 1.8A pulse voltage began at 3.1V and increased to 3.3V. For the remainder of the test the voltage at 17.5A was quite

steady in the range 2.70-2.90V. This cell polarized during the 20th burst, with voltage on both pulse loads dropping, precipitously . The second pair of cells using additive 1 at level B behaved similarly, but polarized during the 22nd duty cycle as shown in Fig. 20. One of these pairs of D cells was then driven into reversal at 1A for 19 hours. During this reversal some cell heating was observed as the cells entered reversal, but no venting or other misbehavior occurred as the cells cooled to room temperature during the reversal.

Two further pairs of D cells with additive 1 level B were also examined on the GLLD duty cycle. The first pair had a very low 17.5A pulse voltage of 0.25 which rose to 2.5 during the three minute burst as shown in Fig. 21. The cell gave a pulse voltage above 2.5V for 17 cycles and polarized badly during the 19th cycle. This pair of cells was then driven into reversal at 1A for 21 hours. The temperature of the cell rose to 54°C as the cell entered voltage reversal, then declined to near room temperature at the end of the discharge. The second pair of cells polarized during the 15th burst as shown in Fig. 22.

Additive 2

Two pairs of cells with additive 2 were tested on the GLLD test cycle. One pair delivered 7 bursts above 2.5V and 16 bursts above 2.0V and did not polarize until the 21st burst as shown in Fig. 23. The pair of cells then ran smoothly in reversal for 19.5 hours. The second pair of cells had load voltage rise from 1.1V to 2.45 in the first burst as shown in Fig. 24. This pair of cells never had a voltage above 2.5V at 17.5A but delivered 19 bursts above 2.0V and polarized during the 24th pulse. This pair of cells was driven 8 hours into reversal at 1A without incident. Maximum measured cell wall temperature was 43°C.

Additive 3

Two pairs of cells fabricated with cathode additive 3 were tested on the GLLD duty cycle. In one case the initial load voltage was 2.5V, rising to 2.85V during the burst. The cell pair delivered 17 bursts over 2.5V and polarized below 2V during the 19th burst as shown in Fig. 25. This cell pair was then driven into reversal for 21 hours at 2A. The cell wall temperature

rose as the cells entered reversal as shown schematically in Fig. 26, but later cooled during the reversal with no venting or other misbehavior. The second pair of cells with additive 3 gave an initial load voltage of 1.20V, rising to 2.75V during the burst. These cells polarized during burst no. 20 as shown in Fig. 27. These cells were also driven into reversal at 2A for 21 hr. with no misbehavior.

Additive 4

One pair of D cells using cathode additive 4 was tested on the GLLD test. The voltage on the initial 17.5A pulse was 0.6, rising to 2.1V in the first burst. The cell polarized during the 21st burst, but load voltage never reached 2.5V and was below 2V after the 12th pulse, as shown in Fig. 28.

Additive 5

One pair of cells using cathode additive 5 has been discharged. The initial pulse voltage of 2.60V rose to 2.85V through the first burst. This cell delivered 16 bursts with a load voltage above 2.5V as shown in Fig. 29 before polarizing very quickly in the 17th pulse.

B. Conclusions

The catalytic additive 1 and 2, both improved the performance of the cells, for example, these cells delivered 20-22 bursts compared to 17-18 brusts realized from cells (9) without any catalytic additive. In view of the fact that the cathodes were unoptimized both with respect to the amount of additive and the manner of impregnation, the 22% increase in performance was rather significant. The abuse resistance of the cells on force-discharge was also significantly improved. Although we did not measure the internal pressure of the cells during the test and the abuse, the fact that the low pressure (130 PSI) vents of these cells remained unopened during both the test and the abuse of the cells, indicate that there was no pressure build-up problem. Therefore, we believe that the approach involving use of catalytic materials in the cathode to improve performance and safety is efficacious.

V. Conclusions and Future Work

The performance of the flat cells, that we developed for the GLLD laser designator application met and exceeded almost all our design goals. The cells had exceedingly low internal impedance and delivered 24-26 bursts above 2.0 volt, with insignificant temperature rise. Although, the assembly of the cells was found to be exceedingly labor intensive at this stage, we plan to continue to optimize the design and assembly procedures of this cell so that in the future these may be made as economically as the spirally wound D cells.

The effort to gain increased understanding of the cell reaction mechanism by cyclic voltammetry, coulometry and spectroscopy , carried out during the first two quarters, paid off handsomely in providing effective approach to improve performance and safety of $Li/SOCl_2$ D cells. Two promising catalytic cathode additives were developed so far. We plan to continue to explore and optimize this approach and incorporate this in flat cells as well in the future.

VI. References

1. W. K. Behl, J. A. Cristopulos, M. Ramirez and S. Gilman, J. Electrochem. Soc., 120, 1619 (1973).

2. J. J. Auborn, K. W. French, S. I. Lieberman, V. K. Shah and A. Heller, ibid, 120, 1613 (1973).

3. D. L. Maricle et al, U. S. Pat. 3, 567, 515 (1971); G. E. Blomgren and M. L. Kornenberg, German Pat. 2, 262, 256 (1973).

4. A. N. Dey and C. R. Schlaikjer, Proc. 26th Power Sources Symposium, Atlantic City, April 1974.

5. C. R. Schlaikjer, U. S. Pat. 4,020,240 (1977), Proc. 28th Power Sources Symposium, Atlantic City, June 1978.

6. J. P. Gabano and P. Lenfant, Abstract No. 27, Electrochemical Society Meeting, Pittsburg, PA., Oct. 1978.

7. A. N. Dey, "Sealed Primary Lithium Inorganic Electrolyte Cell" Final Report, DELET-TR-74-0109-F, P.R. Mallory & Co., Inc. July 1978.

8. A. N. Dey, W. Bowden, J. Miller, P. Witalis, "Lithium-Thionyl Chloride Battery", ERADCOM, DELET-TR-78-0563-1, First Quarterly Report, P. R. Mallory & Co. Inc., April, 1979.

9. A. N. Dey, W. Bowden, J. Miller, P. Witalis, "Lithium-Thionyl Chloride Battery", ERADCOM, DELET-TR-78-0563-2, Second Quarterly Report, P. R. Mallory & Co. Inc., July, 1979.

10. A. N. Dey and P. Bro, Proc. Brighton Power Sources Symposium (1976), p. 508.

TABLE 1

Short-Circuit Currents of the Experimental Flat Cylindrical Cells with Various Cathode Designs

	Cathode Current Collector Design	Short Circuit Current (A)	Short Circuit Current Densities (mA/cm^2)
1.	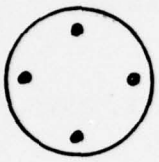	7.0	176
2.	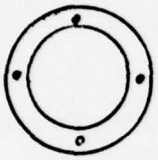 (10 mil)	8.0	201
3.	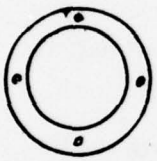 (5 mil)	7.4	186
4.	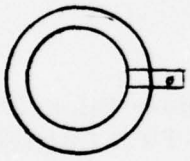	8.6	216
5.	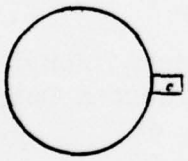	6.2	156
6.	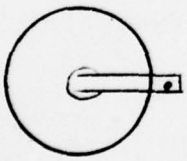	9.2	231
7.	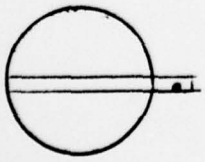	8.8	221
8.	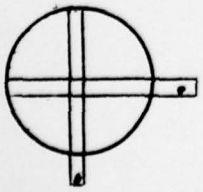	7.2	181

TABLE 2

Performance of High Rate $Li/SOCl_2$ D Cells on GLLD

And Modified GLLD Tests at Room Temperature

Cathode Configuration		LOAD VOLTAGE ON 17.5A	
		Bursts Above 2.5V	Bursts Above 2.0V
A	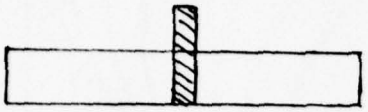 20"	9 16* 11**	11 16* 11**
B	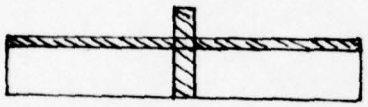 20"	9*	10*
C	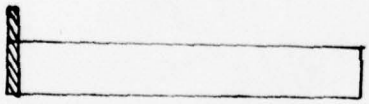 25"	1**	4**
D	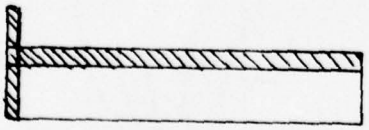 25"	8* 7** 12*	10* 7* 12*
E	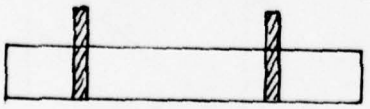 25"	16* 11**	16* 11**
F	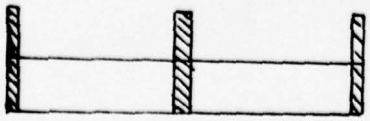 25"	17 16* 11**	17 16* 11**

* Modified GLLD Test at 6.5A

** Modified GLLD Test at 8A

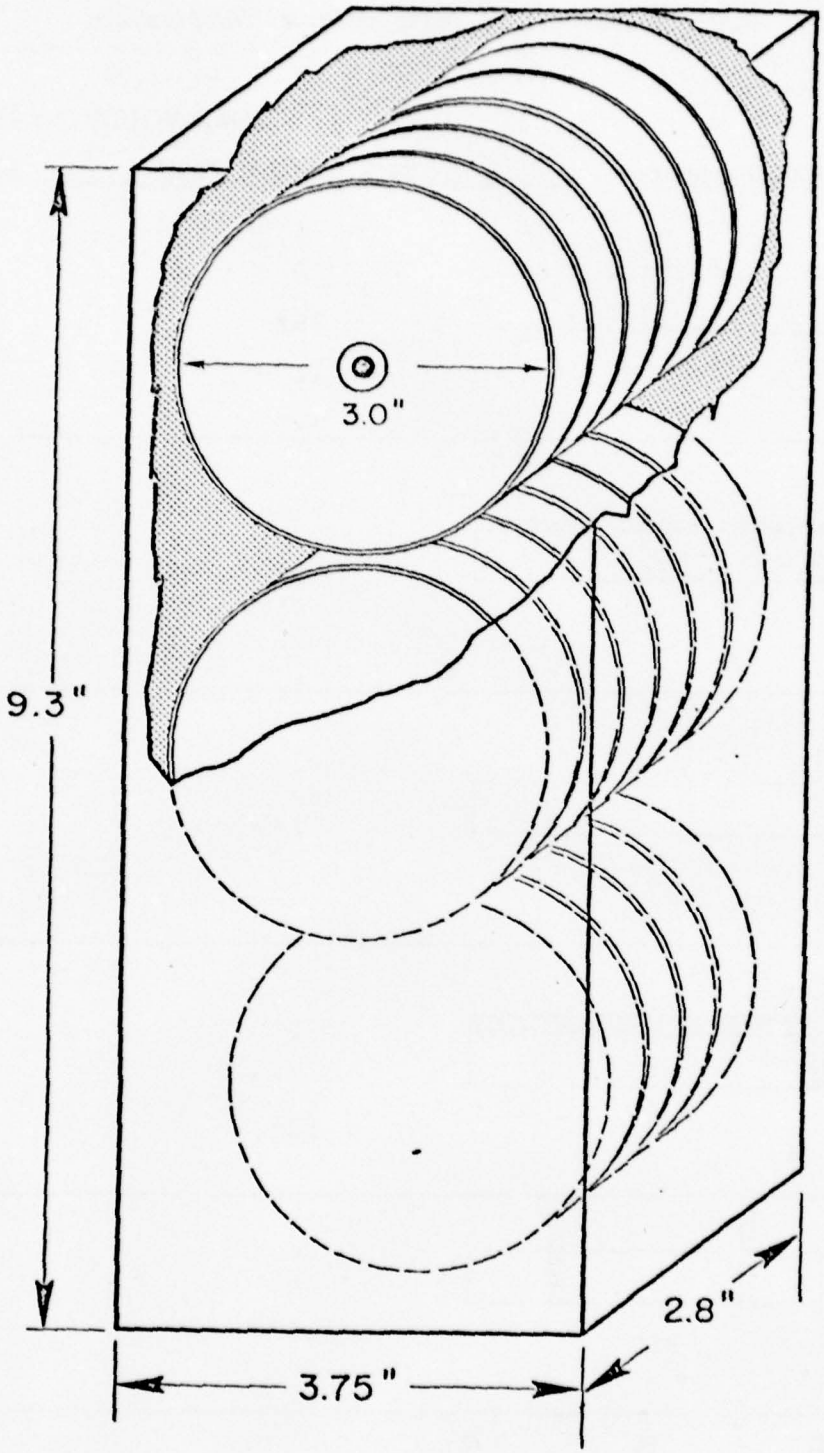

Fig. 1 Laser designator battery with thin flat cells

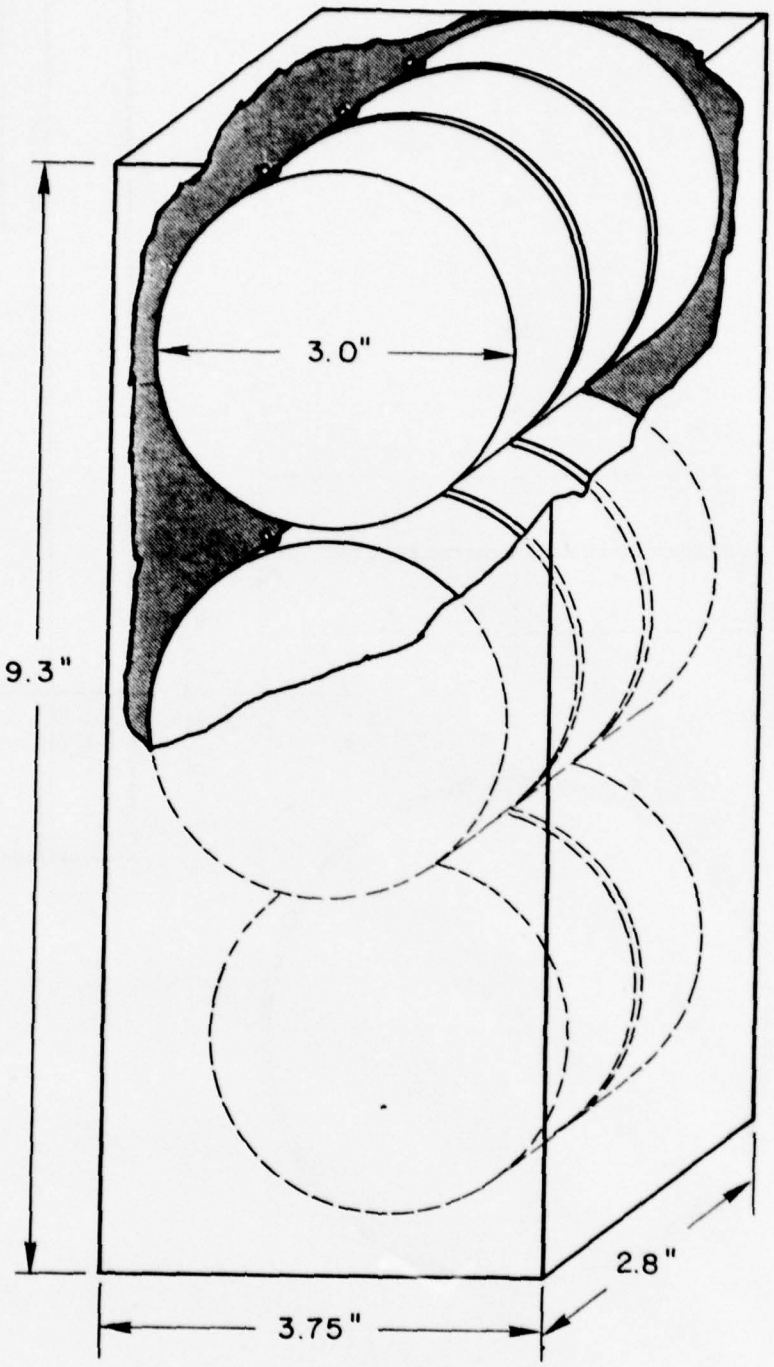

Fig. 2 Laser designator battery with thick flat cells

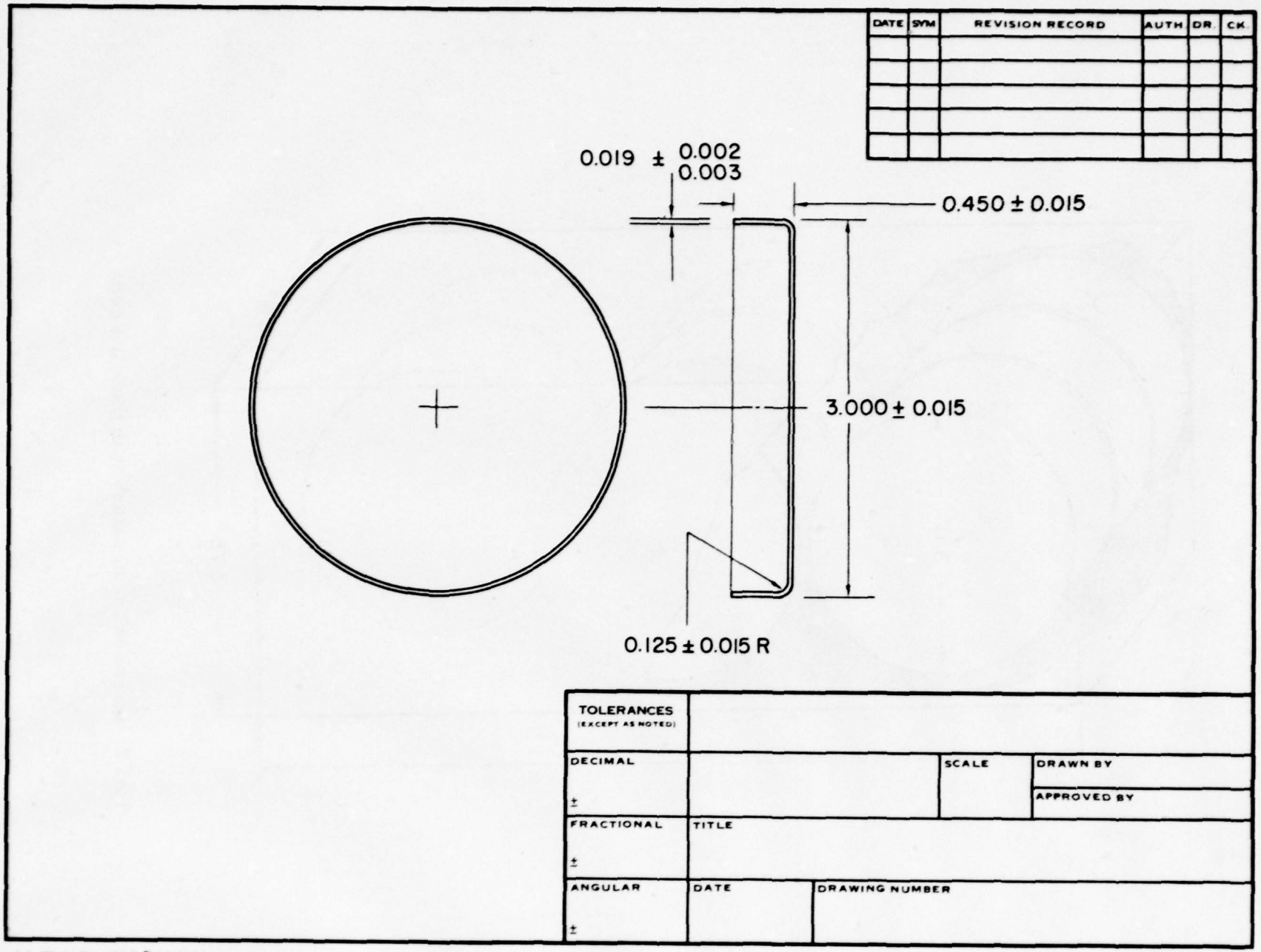

Fig. 3 Flat cylindrical cell container

DATE	SYM	REVISION RECORD	AUTH	DR	CK.

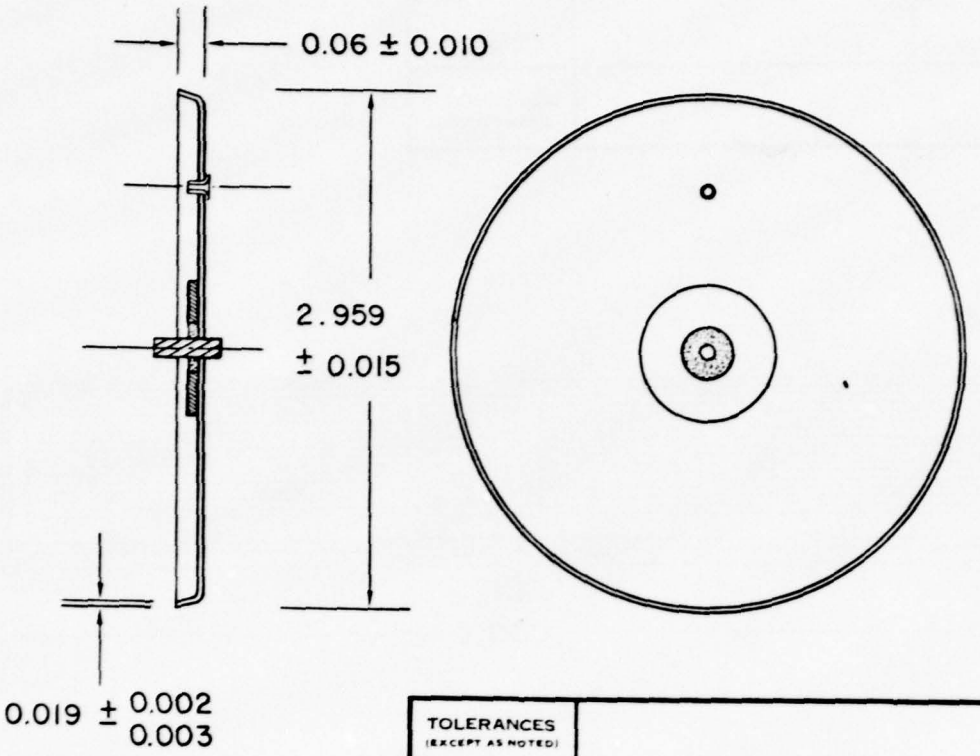

TOLERANCES (EXCEPT AS NOTED)			
DECIMAL ±		SCALE	DRAWN BY / APPROVED BY
FRACTIONAL ±	TITLE		
ANGULAR ±	DATE	DRAWING NUMBER	

K·E ALBANENE ® 10 5465 ENGINEERS' STANDARD FORM

Fig. 4 Flat cylindrical cell top with G/M seal and the electrolyte fill port

MADE IN U.S.A.

DATE	SYM	REVISION RECORD	AUTH	DR	CK

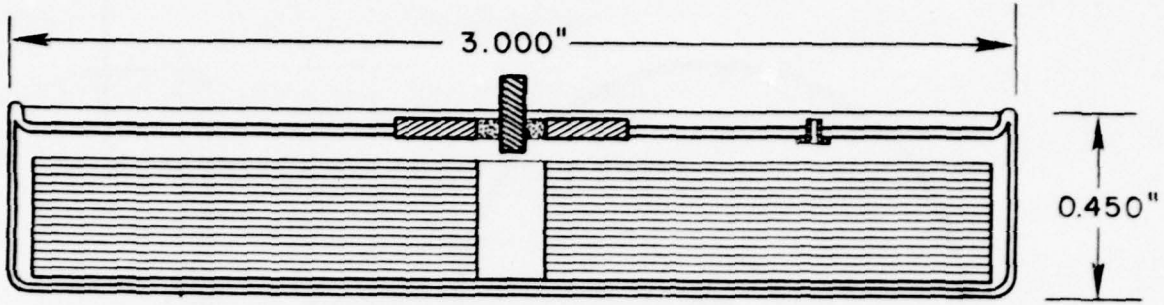

TOLERANCES (EXCEPT AS NOTED)			
DECIMAL ±		SCALE	DRAWN BY
			APPROVED BY
FRACTIONAL ±	TITLE		
ANGULAR ±	DATE	DRAWING NUMBER	

K•E ALBANENE ® 10 5465 ENGINEERS' STANDARD FORM

MADE IN U.S.A.

Fig. 5 Cross-Section of the hermetic flat cylindrical cell

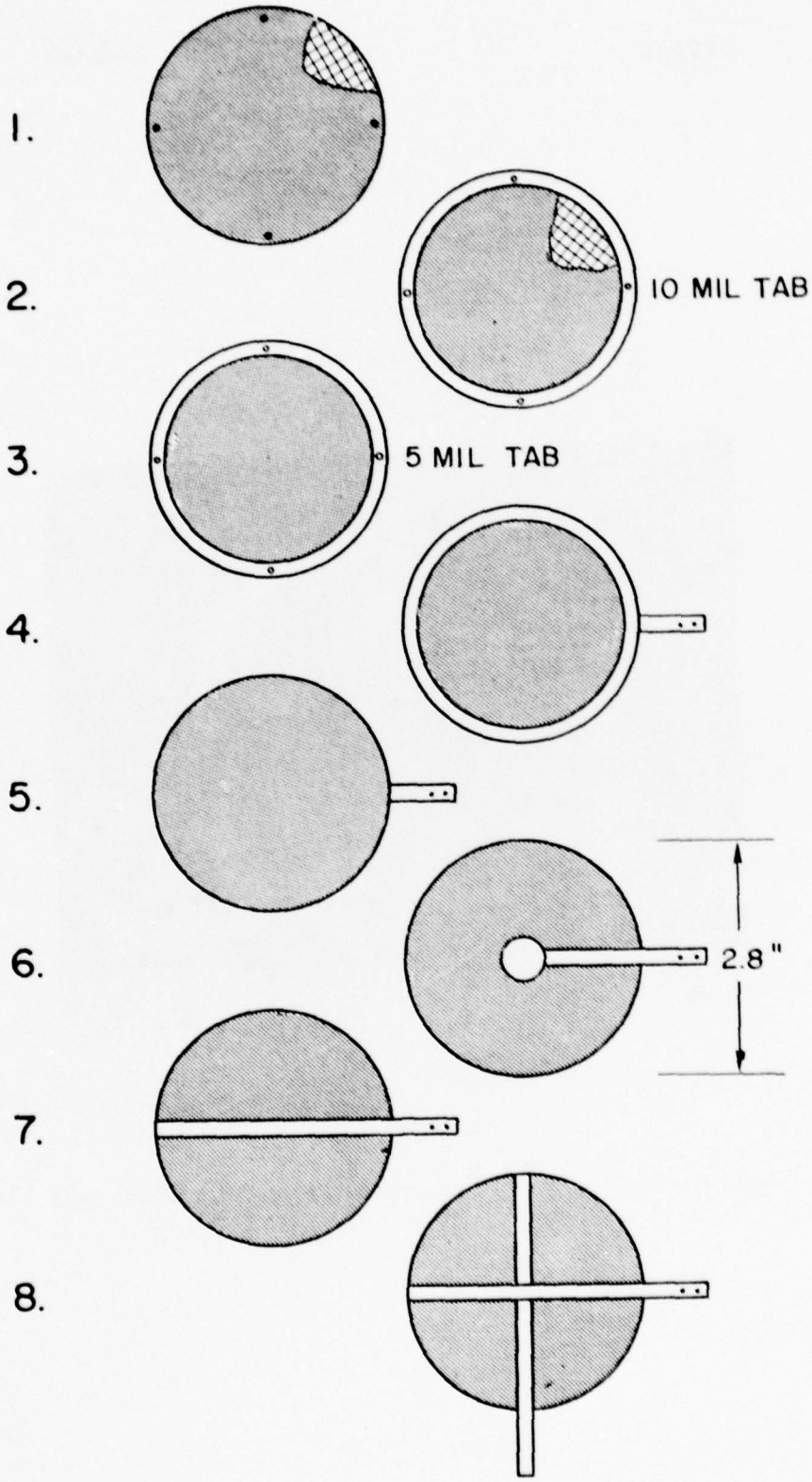

Fig. 6 Current collector designs for the 2.8 inch diameter disc cathodes

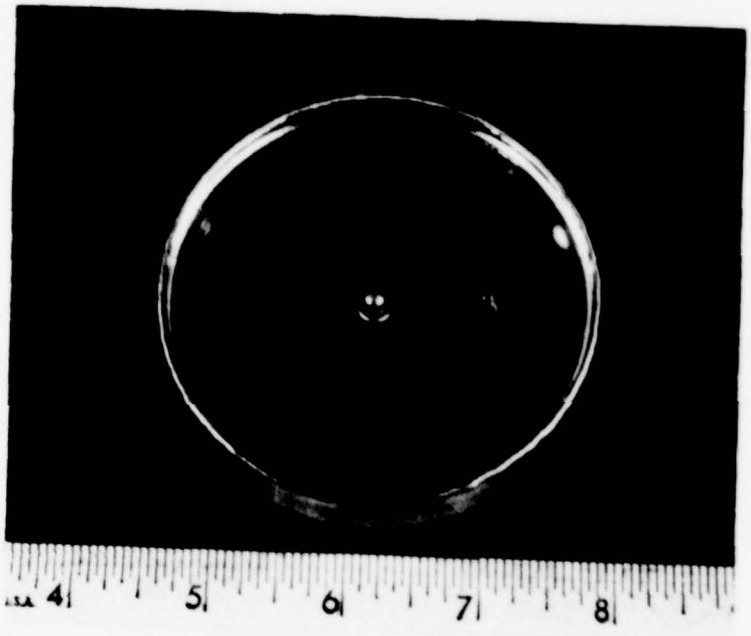

Fig. 7 Photograph of a hermetic flat cylindrical cell

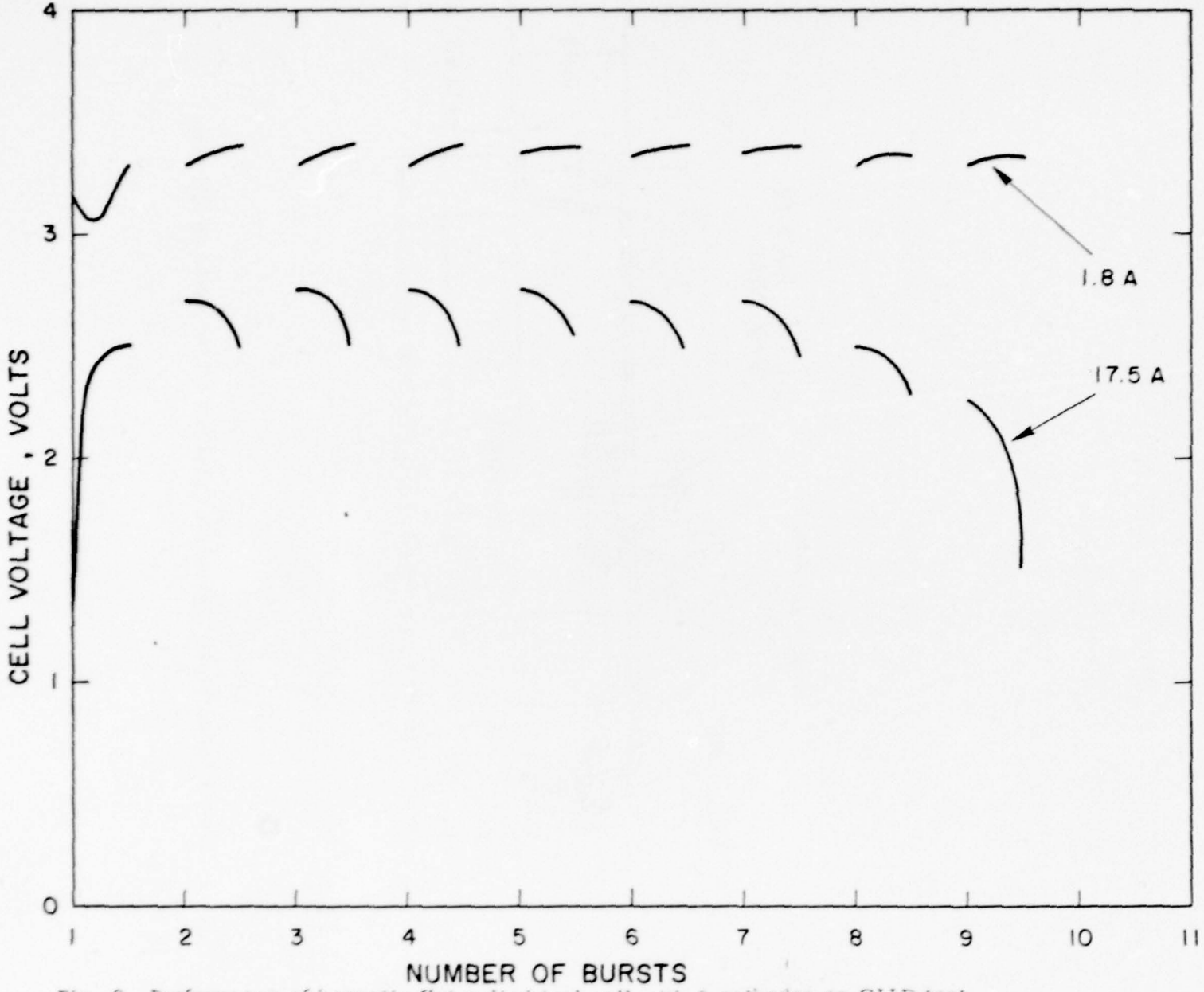

Fig. 8 Performance of hermetic flat cylindrical cell with 8 cathodes on GLLD test

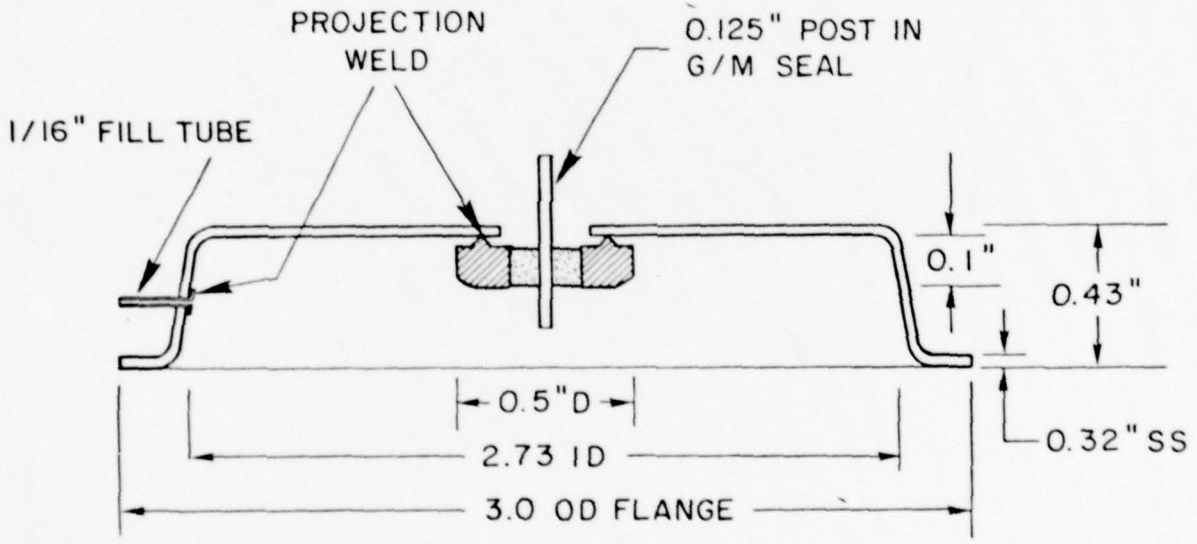

Fig. 9 Top of hermetically sealed flat cell with G/M seal and fill tube

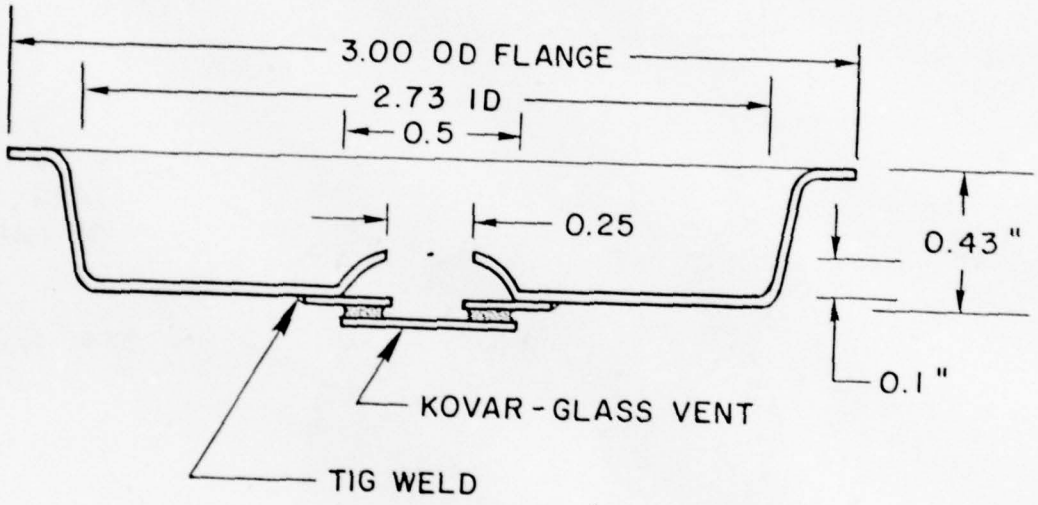

Fig. 10 Bottom of hermetically sealed flat cell showing low pressure G/M seal vent

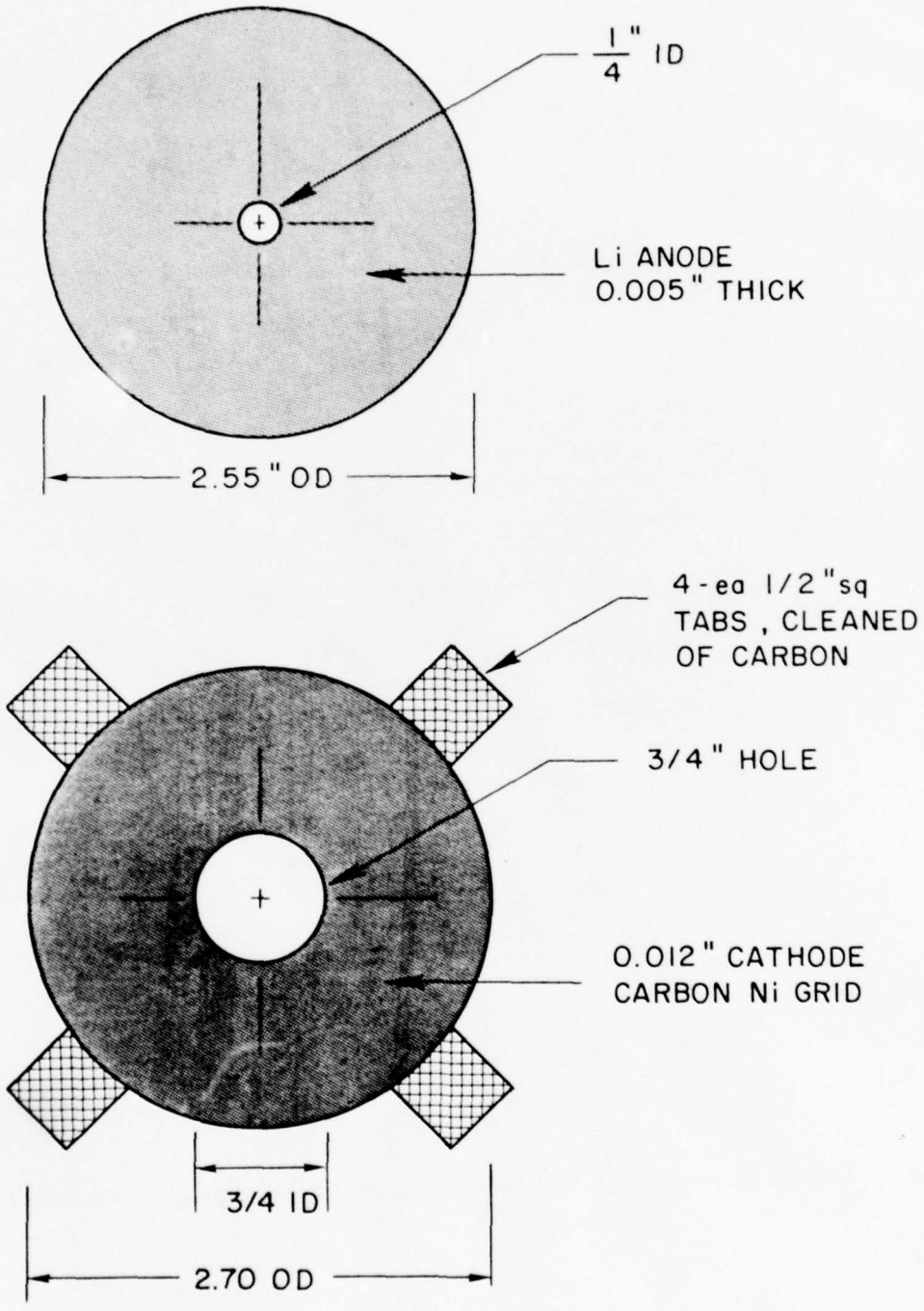

Fig. 11 The anode and cathodes for a flat cell

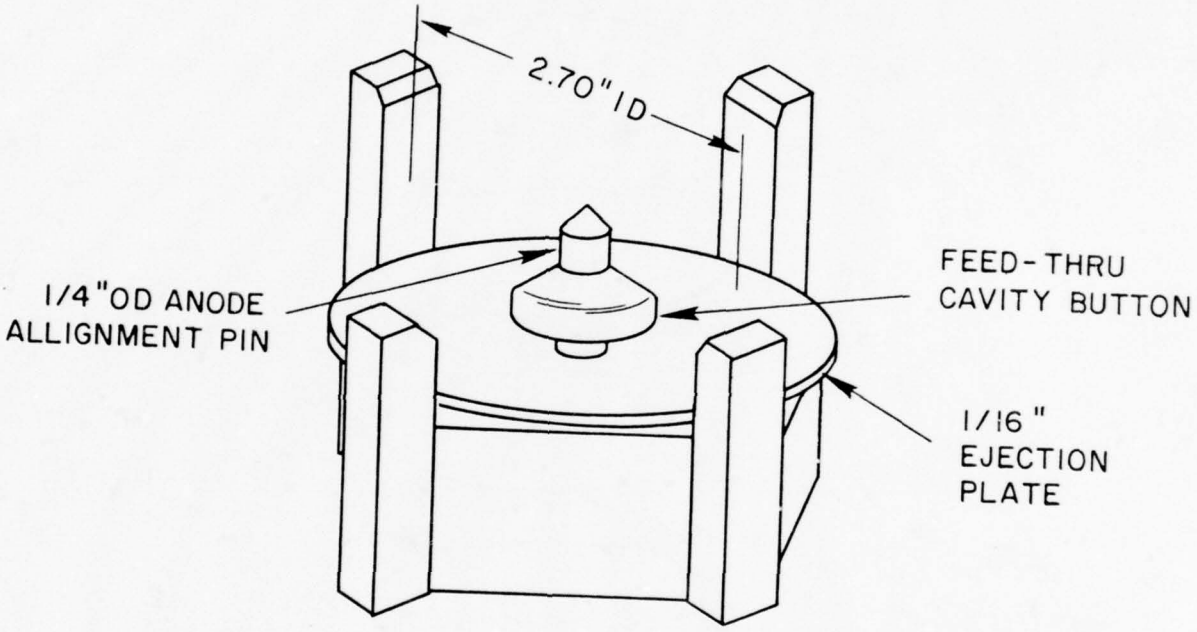

Fig. 12 The flat cell assembly fixture

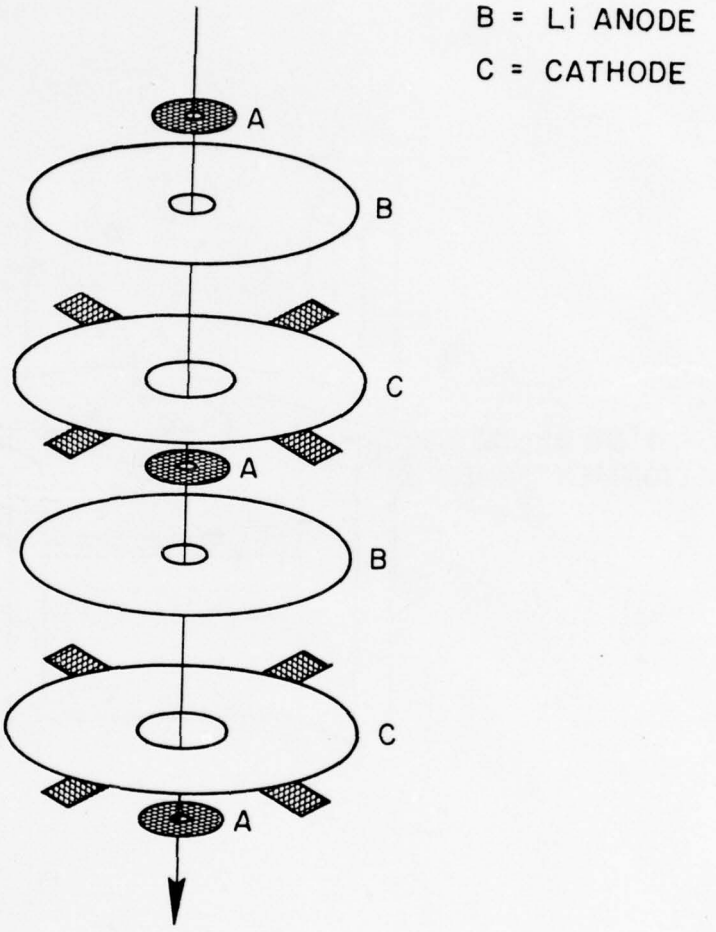

Fig. 13 Assembly stacking sequence for the flat cell

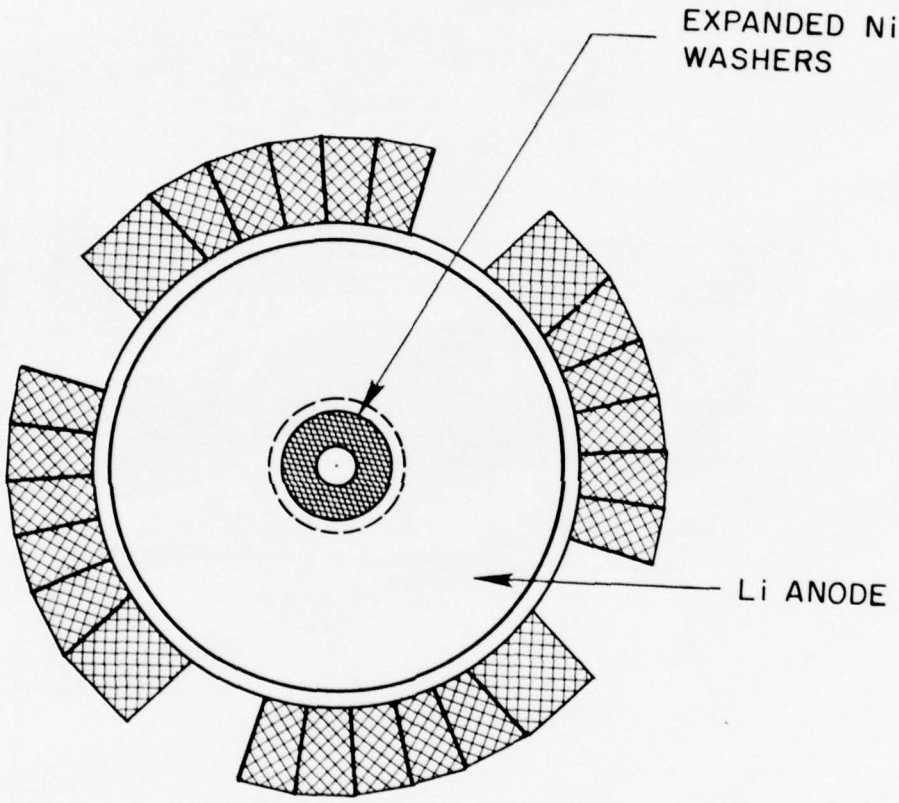

Fig. 14 Top view of an assembled flat cell

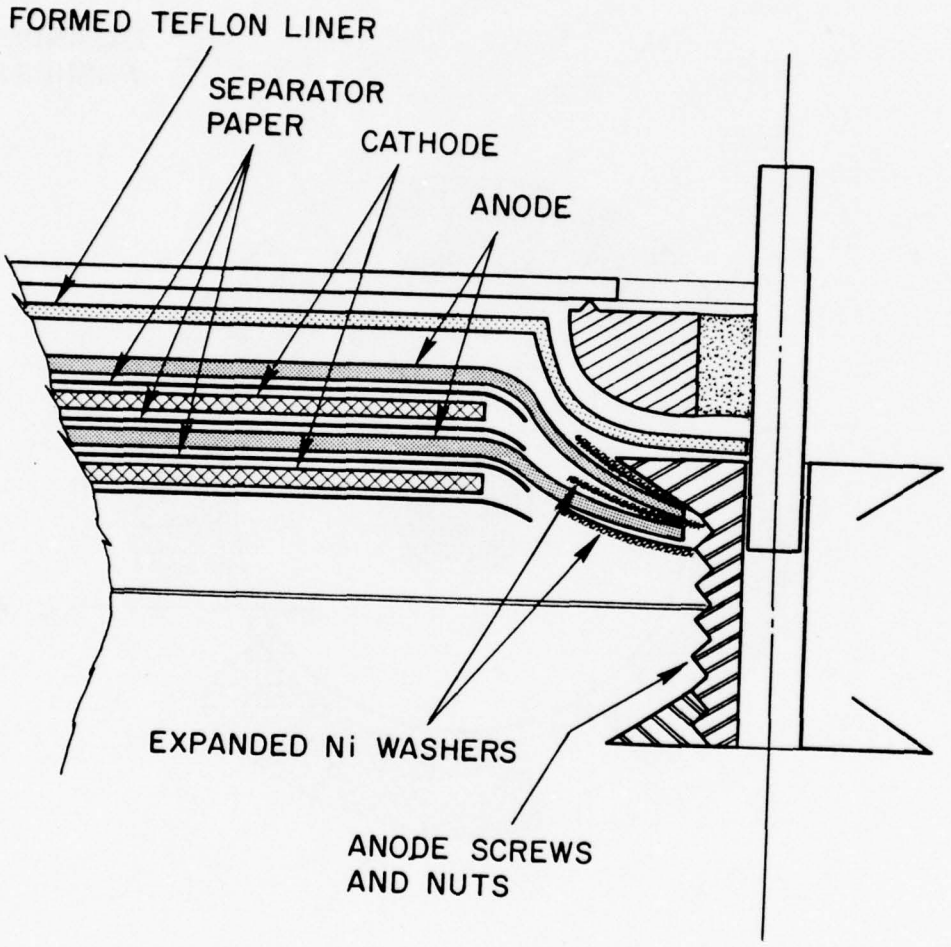

Fig. 15 Lithium anode contact detail

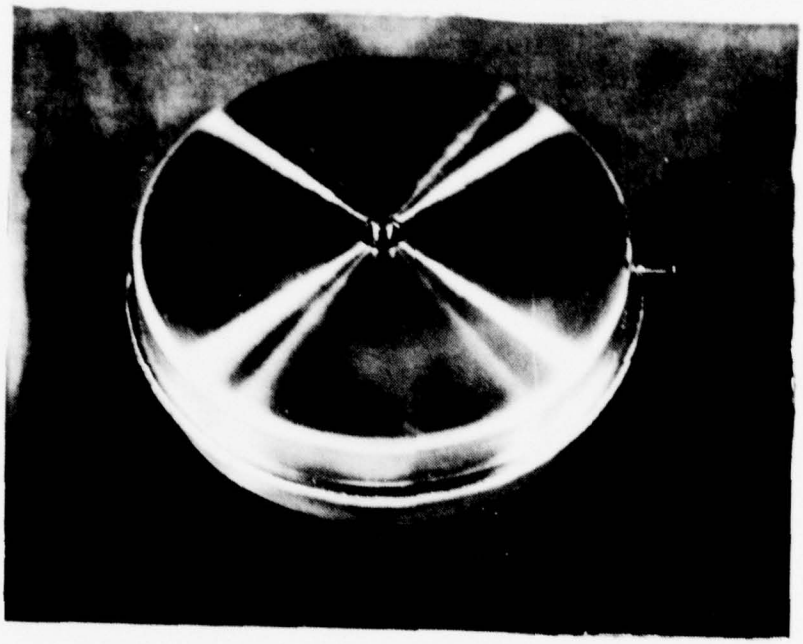

Fig. 16 Photograph of finished flat cell

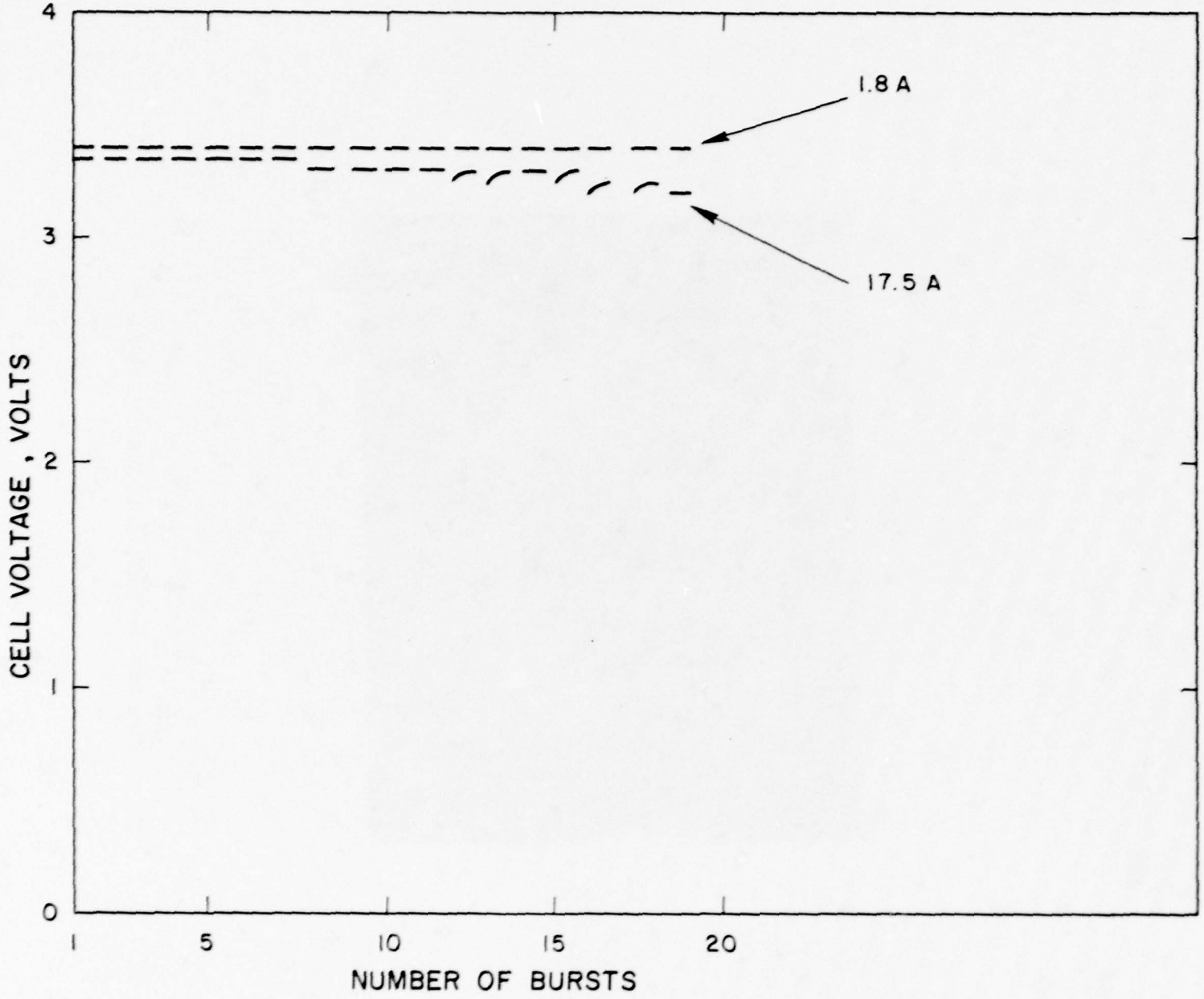

Fig. 17 Performance of flat cell on GLLD test cycle

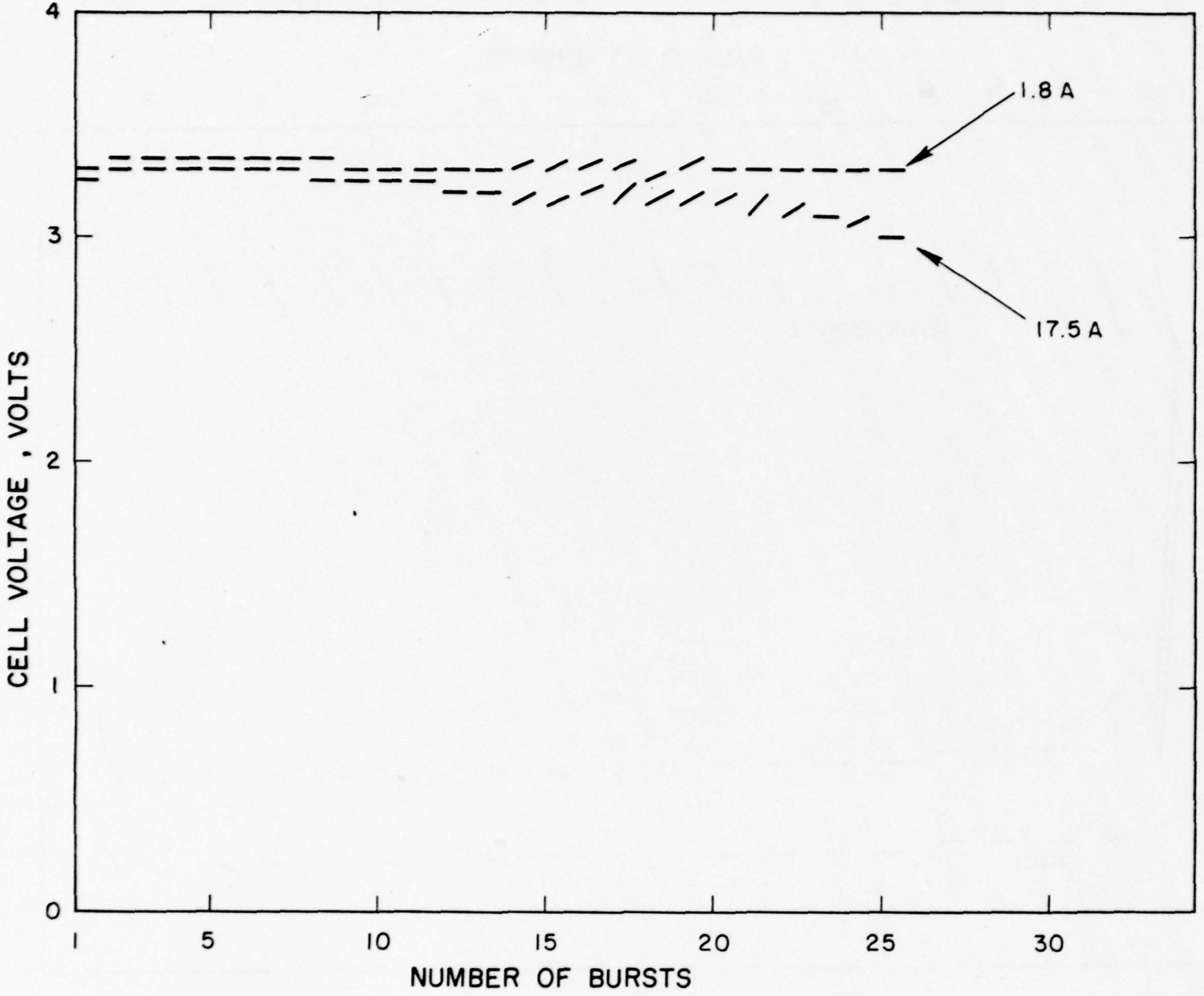

Fig. 18 Performance of flat cell on GLLD test cycle

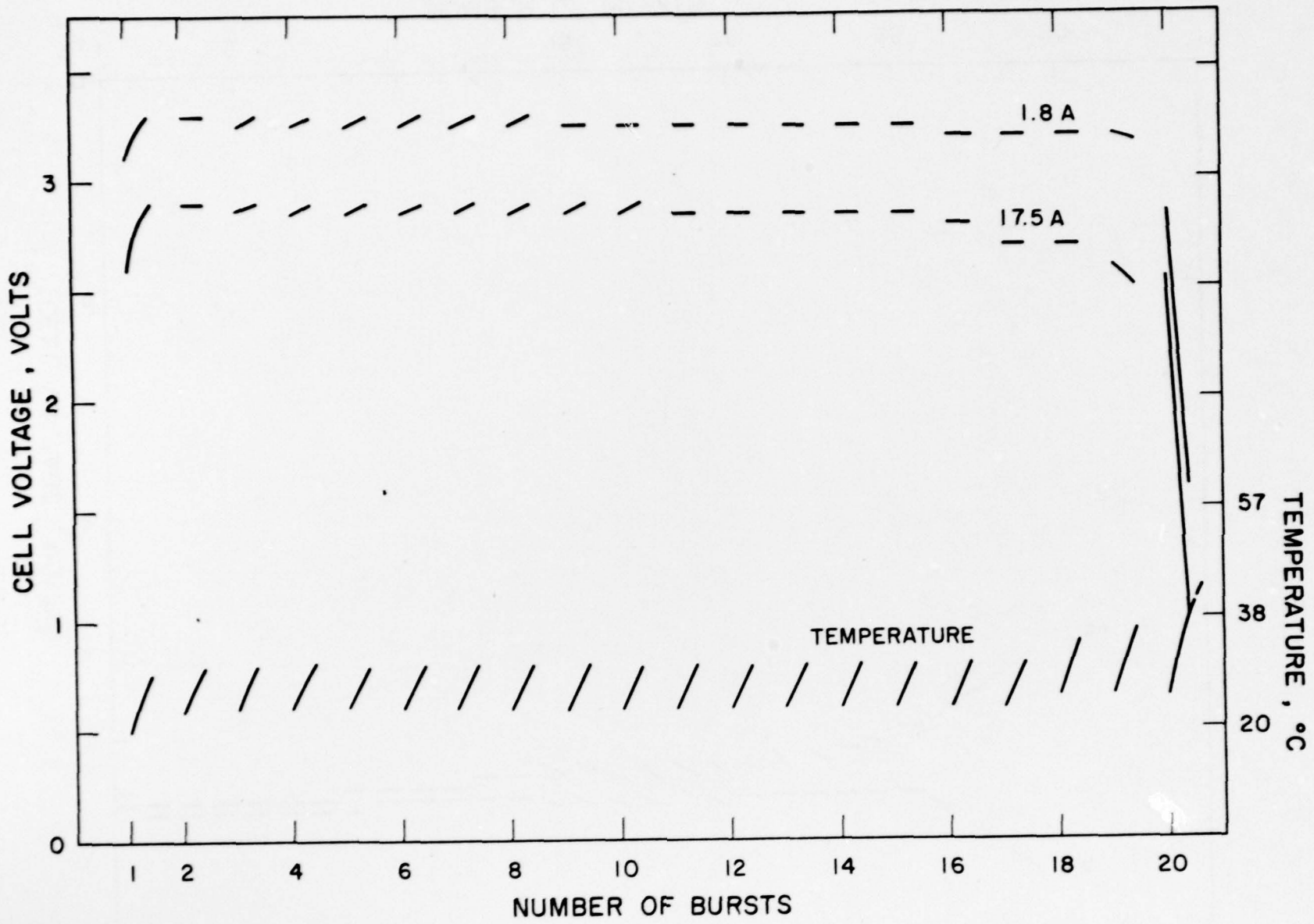

Fig. 19 Performance of two D cells with cathode additive, level A on GLLD test

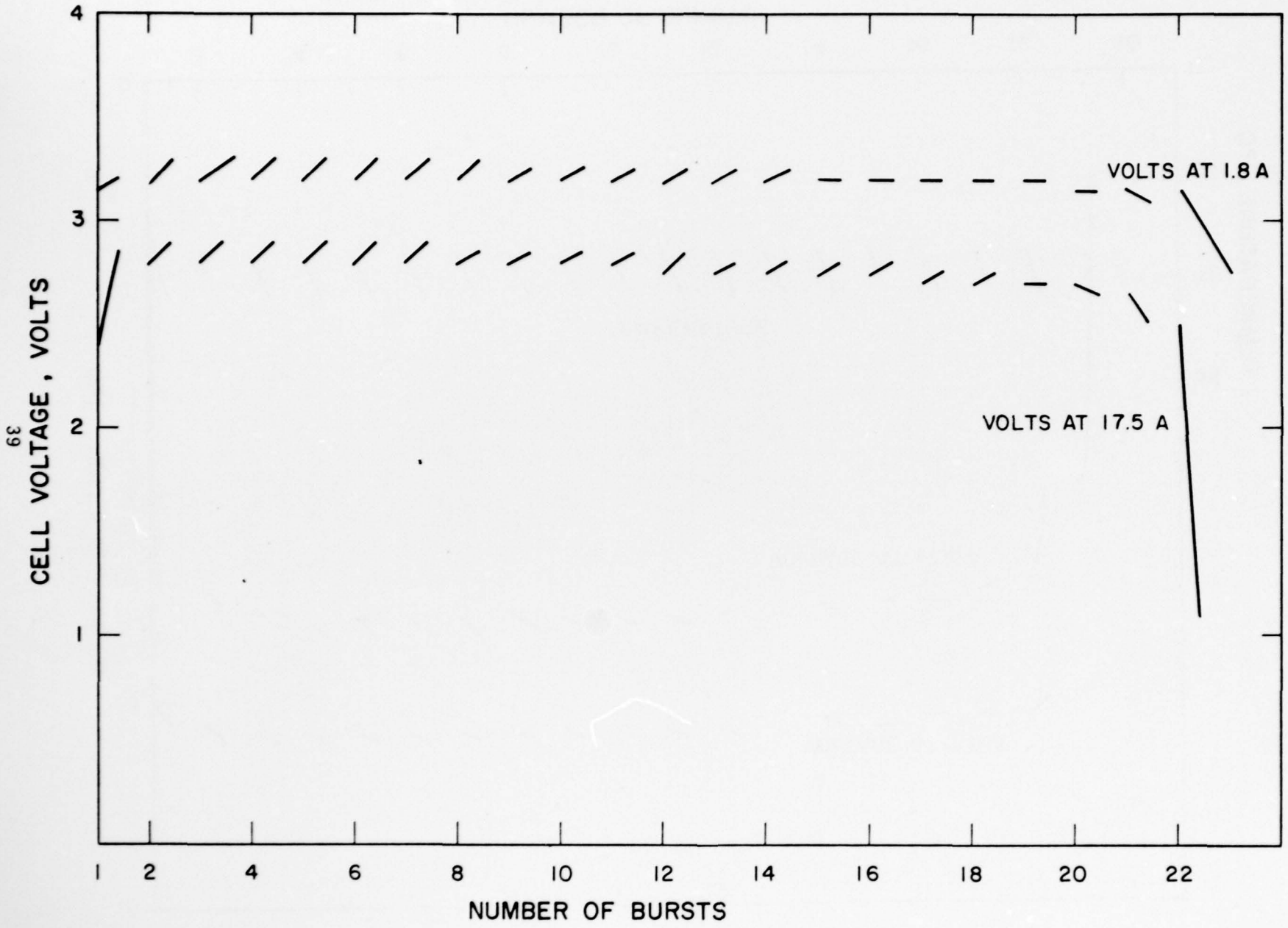

Fig. 20 Performance of two D cells with cathode additive 1, level A on GLLD test

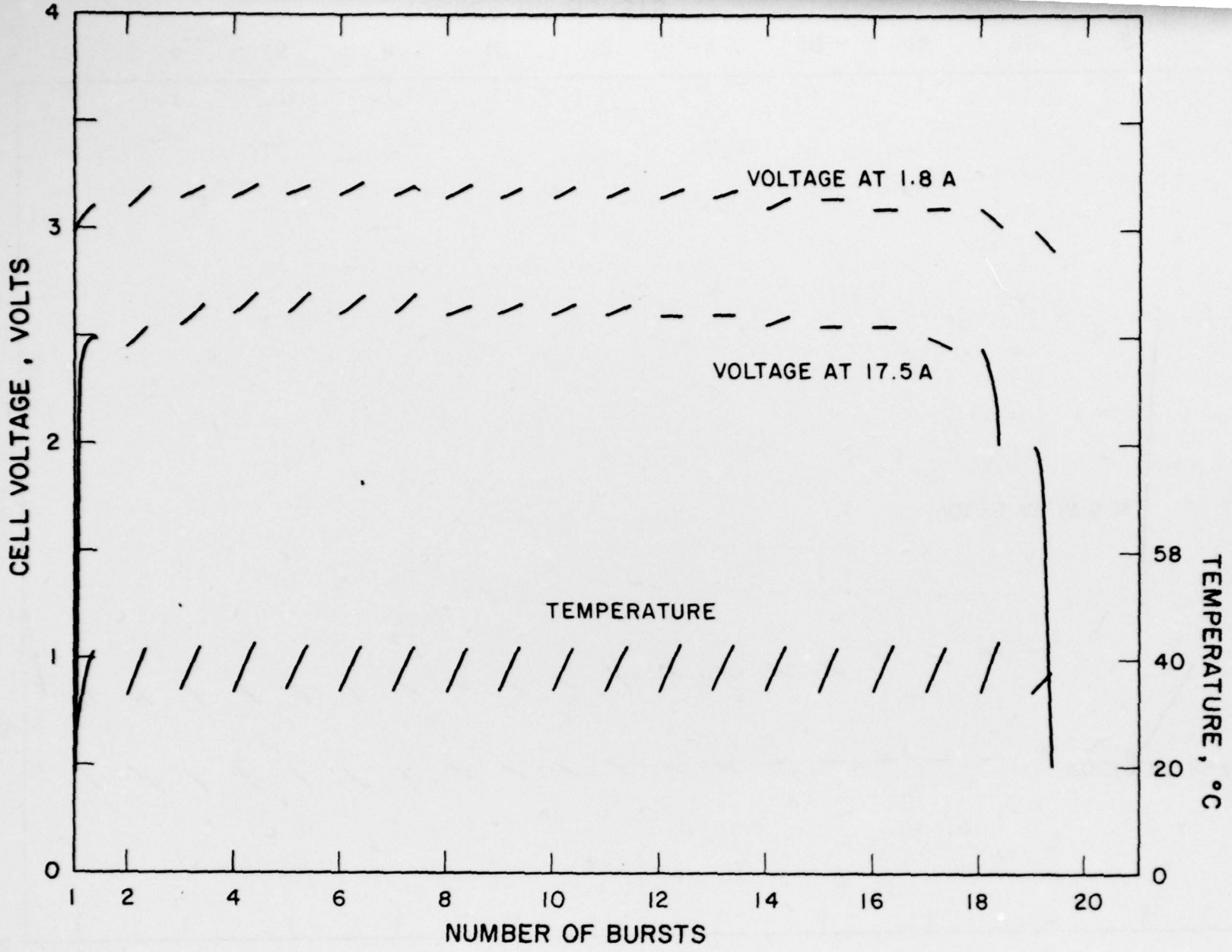

Fig. 21 Performance of two D cells with cathode additive 1, level B on GLLD test

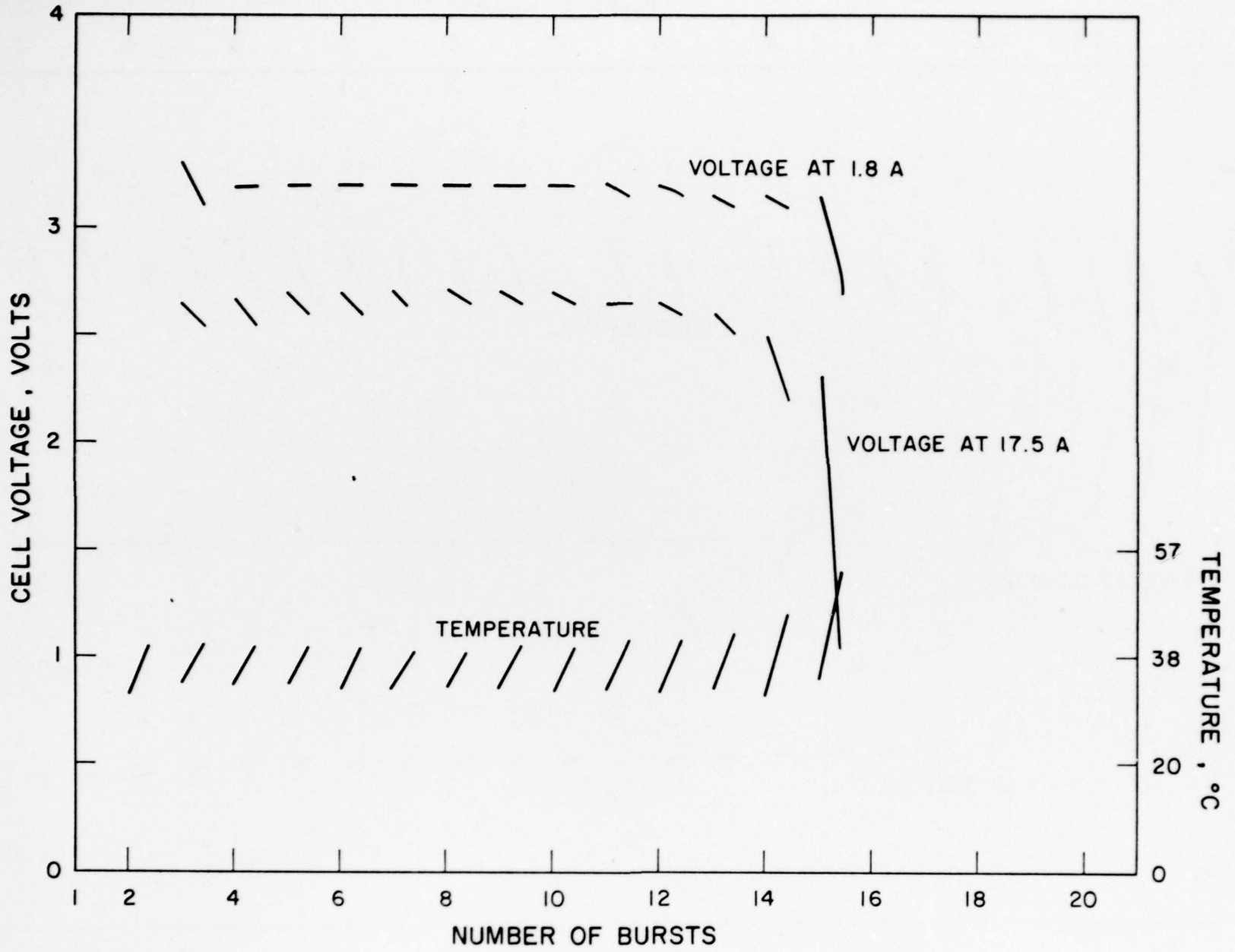

Fig. 22 Performance of two D cells with cathode additive 1, level B on GLLD test

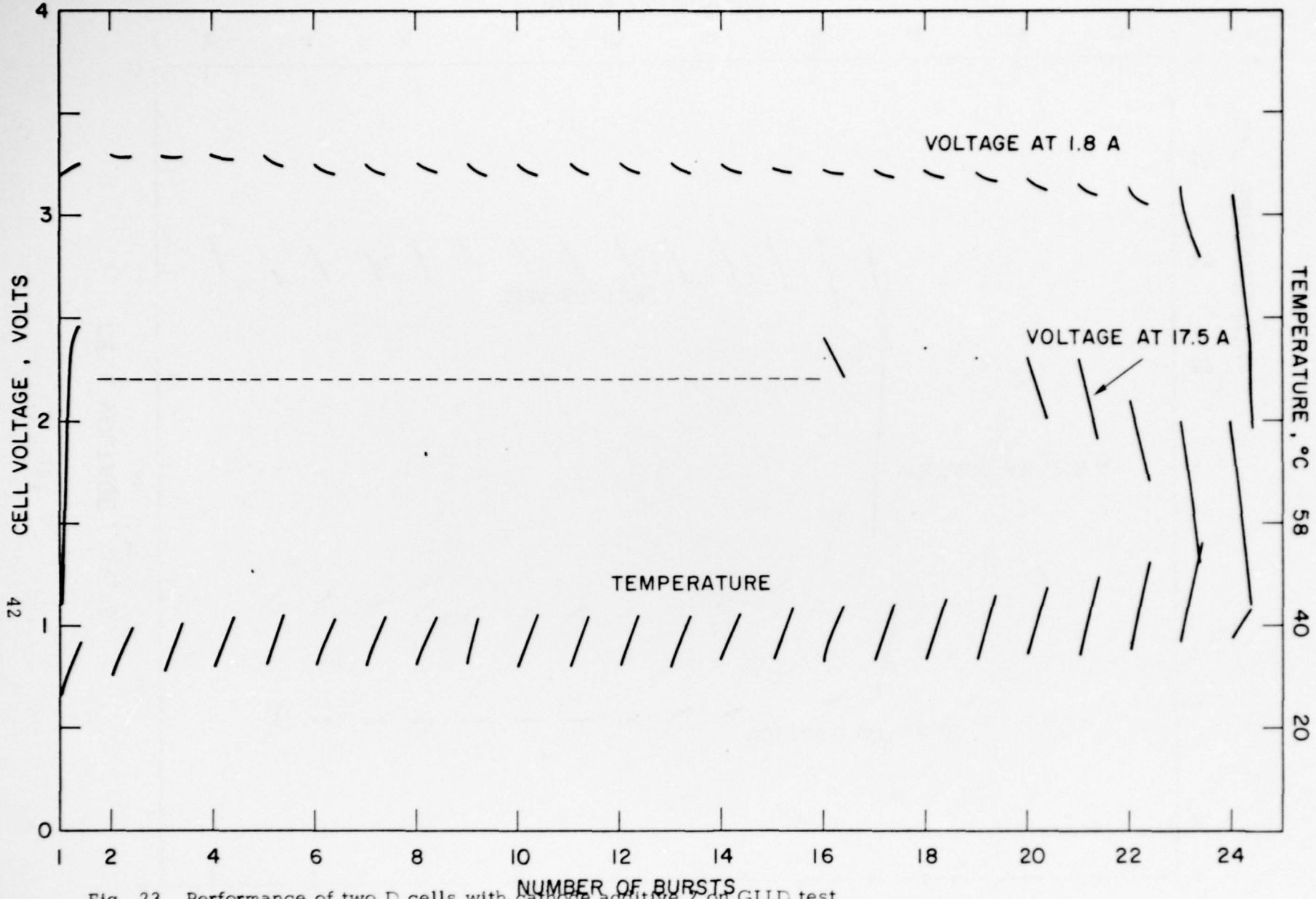

Fig. 23 Performance of two D cells with cathode additive 2 on GLLD test

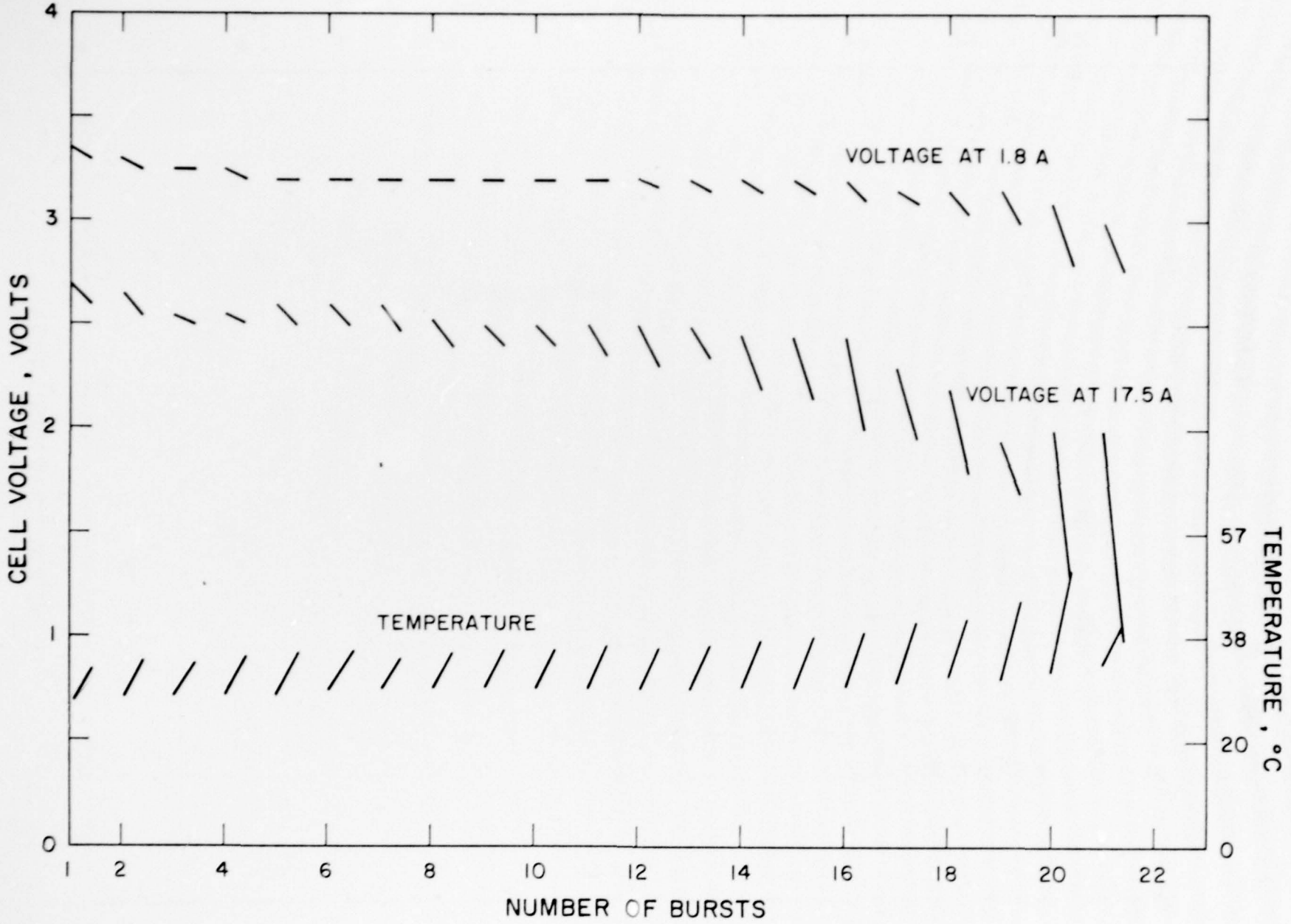

Fig. 24 Performance of two D cells with cathode additive 2 on GLLD test

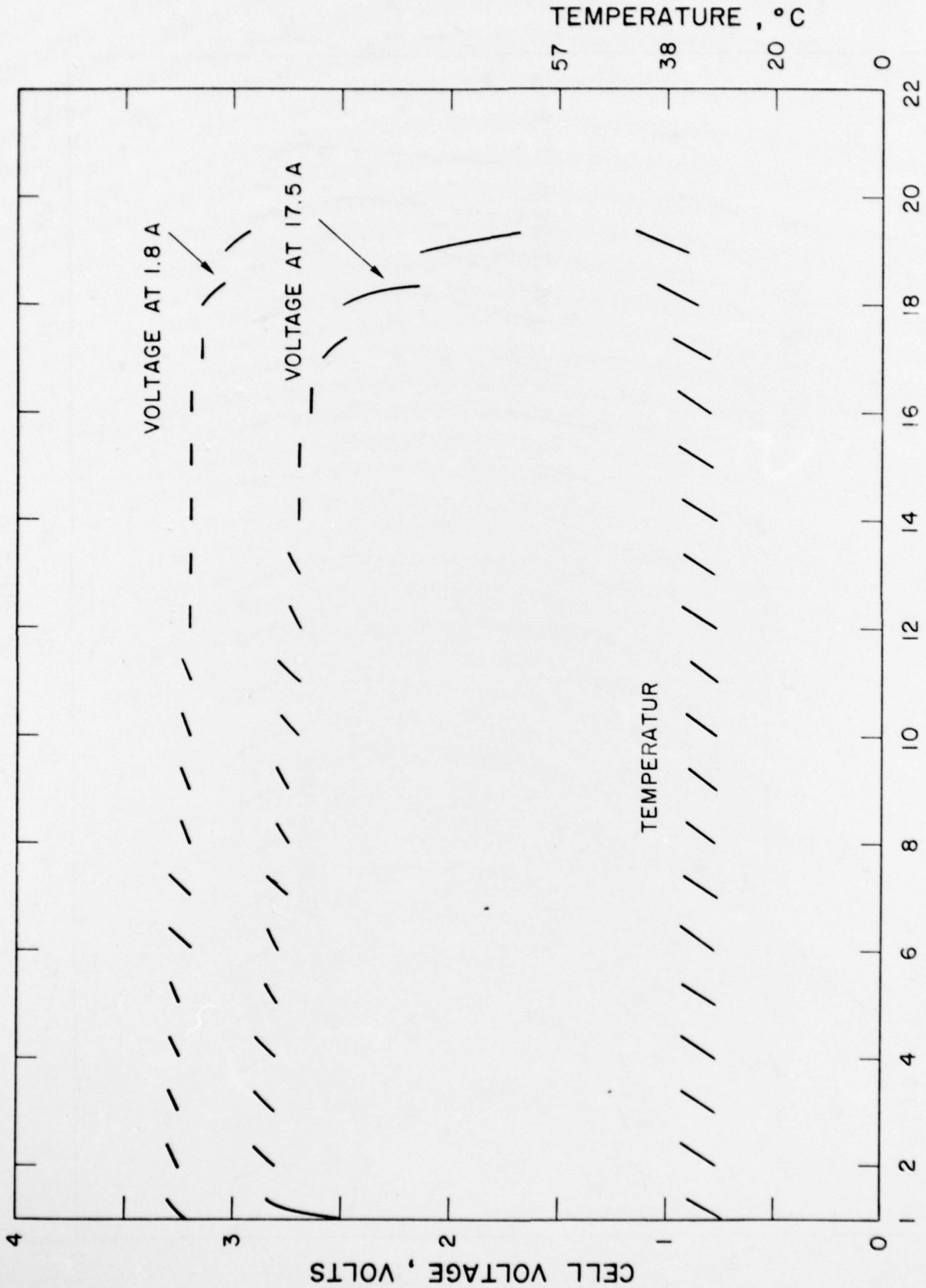

Fig. 25 Performance of two D cells with cathode additive 3 on GLLD test

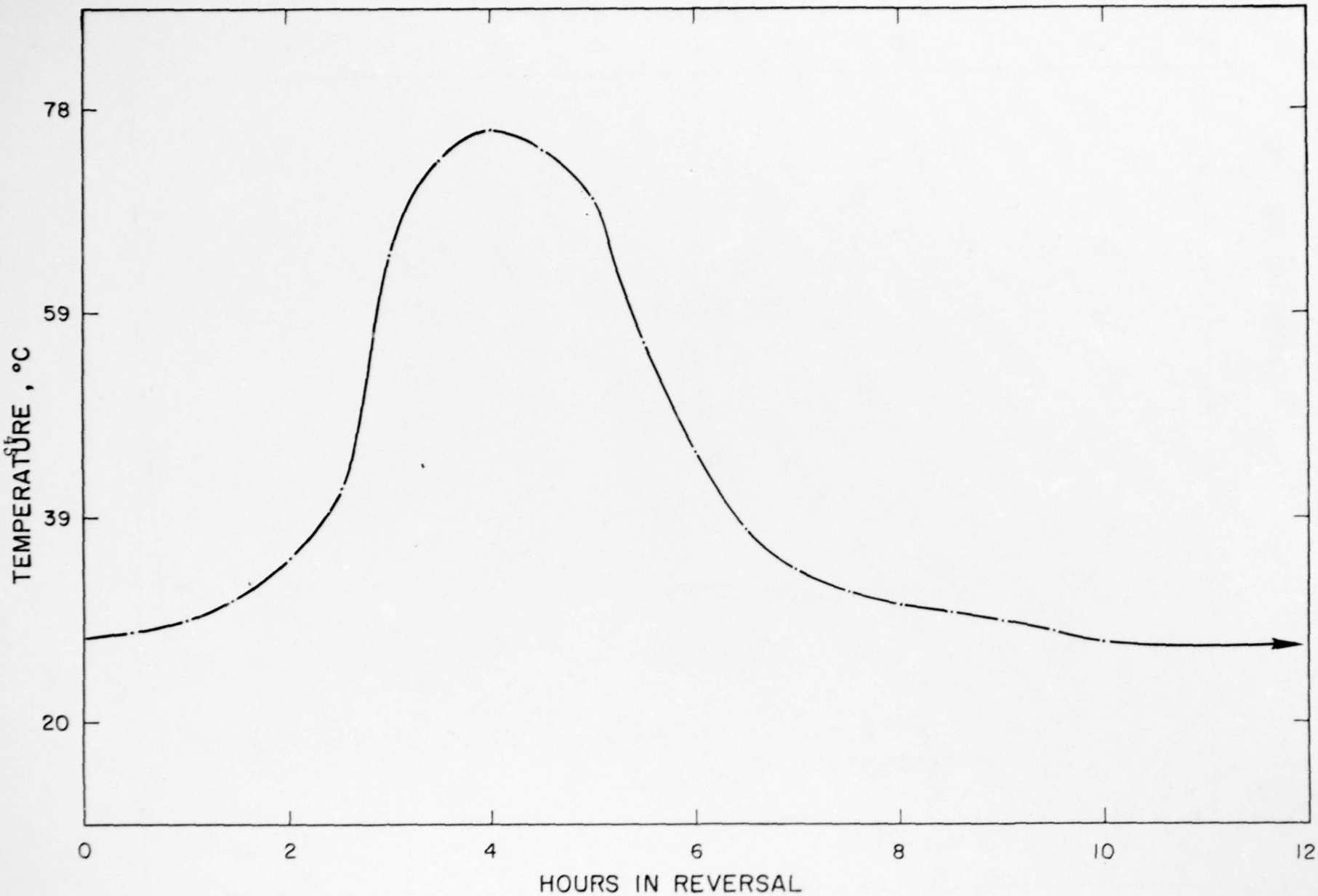

Fig. 26 Cell wall temperature of 2 D cells with cathode additive 3 during reversal at 2A

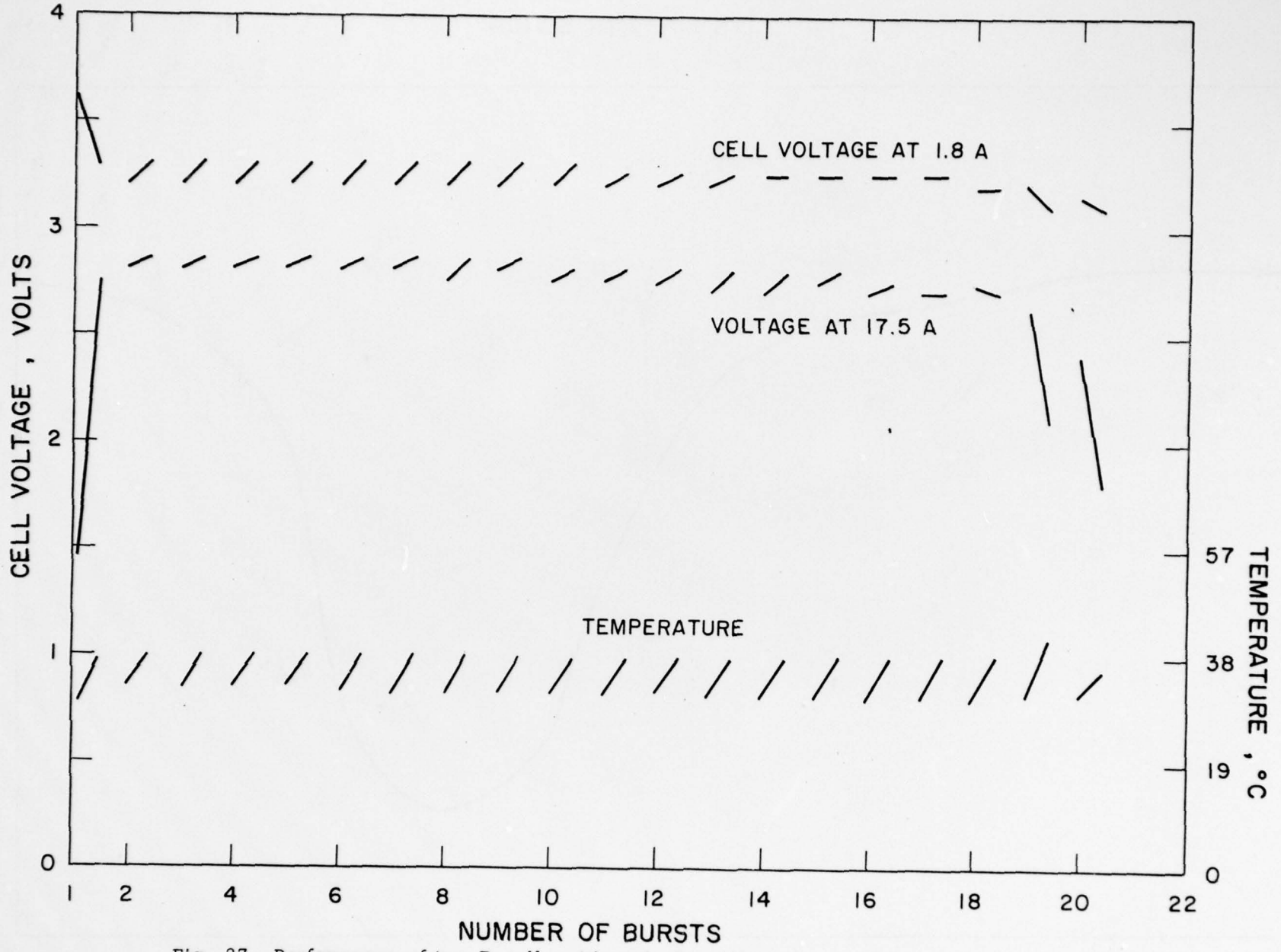

Fig. 27 Performance of two D cells with cathode additive 3 on GLLD test

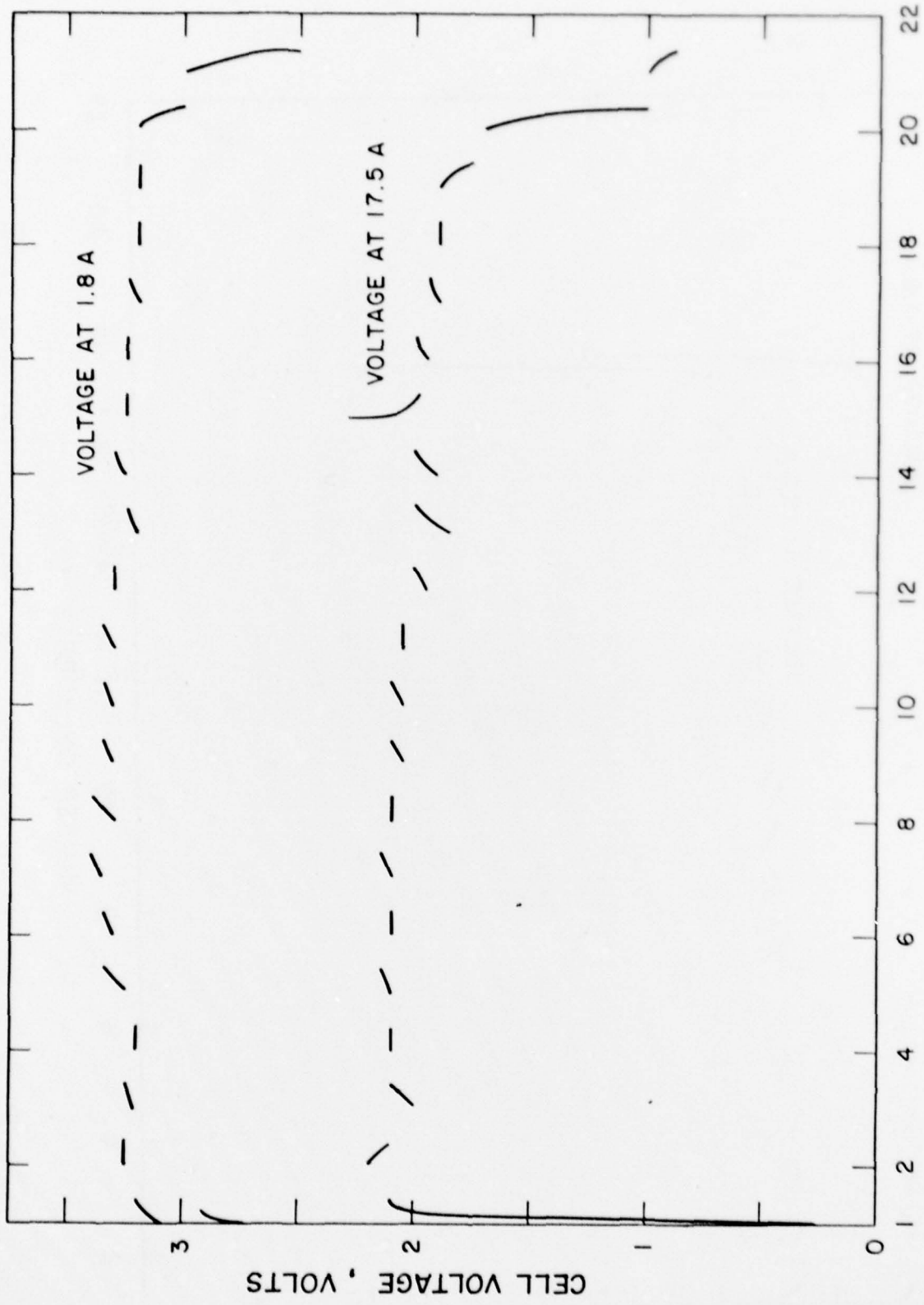

Fig. 28 Performance of two D cells with cathode additive 4 on GLLD test

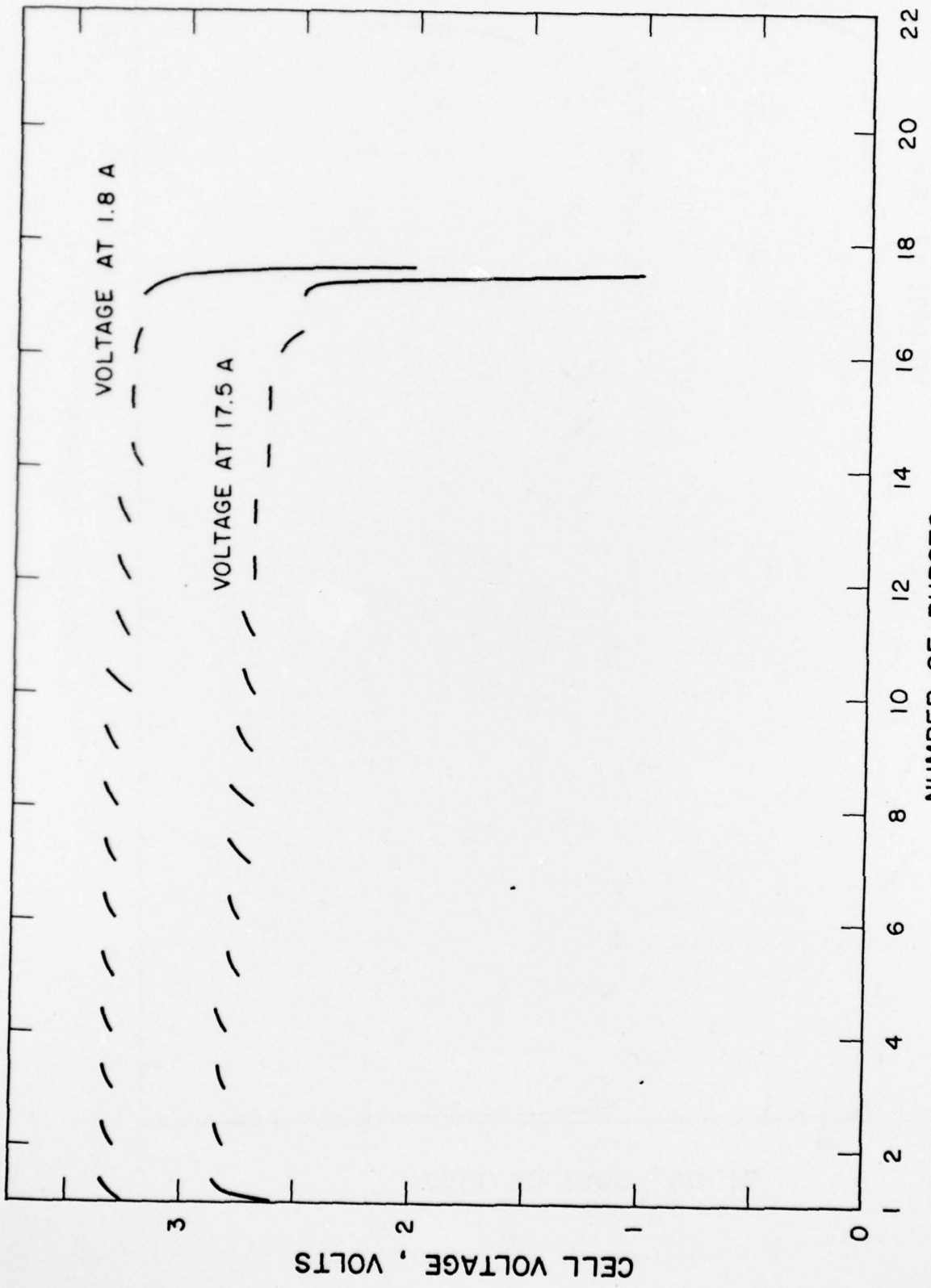

Fig. 29 Performance of two D cells with cathode additive 5 on GLLD test

ELECTRONICS TECHNOLOGY AND DEVICES LABORATORY

DISTRIBUTION LIST

1 Feburary 1979

Defense Documentation Center (12)
ATTN: DDC-TCA
Cameron Station (Bldg 5)
Alexandria, VA 22314

Commander (1)
Naval Ocean Systems Center
ATTN: Library
San Diego, CA 92152

CDR, Naval Surface Weapons Center (1)
White Oak Laboratory
ATTN: Library Code WX-21
Silver Spring, MD 20910

Commandant, Marine Corps (2)
HQ US Marine Corps
ATTN: Code LMC
Washington, DC 20380

Rome Air Development Center (1)
ATTN: Documents Library (TILD)
Griffiss AFB, NY 13441

Air Force Geophysics LAB/SULL (1)
ATTN: S-29
Hanscom AFB, MA 01731

HQDA (DAMA-ARZ-D) (1)
Dr. F. D. Verderame
Washington, DC 20310

CDR, Harry Diamond Laboratories (1)
ATTN: Library
2800 Powder Mill Road
Adelphi, MD 21783

Director (1)
US Army Materiel Systems Analysis Actv
ATTN: DRXSY-MP
Aberdeen Proving Ground, MD 21005

CRD, US Army Research Office (1)
ATTN: DRXRO-IP
PO Box 12211
Research Triangle Park, NC 27709

CDR, US Army Signals Warfare Lab (1)
ATTN: DELSW-OS
Vint Hill Farms Station
Warrenton, VA 22186

Commander (1)
US Army Mobility Eqp Res & Dev CMD
ATTN: DRDME-R
Fort Belvoir, VA 22160

Commander
US Army Electronics R&D Command
Fort Monmouth, NJ 07703

DELET-P	(1)
DELET-DD	(1)
DELET-DT	(2)
DELSD-L (Tech Lib)	(1)
DELSD-L-S (STINFO)	(2)
DELET-PR	(5)

Commander
US Army Communications R&D Command
Fort Monmouth, NJ 07703

USMC-LNO	(1)

NASA Scientific & Tech Info Facility (1)
Baltimore/Washington Intl Airport
PO Box 8757, MD 21240

SUPPLEMENT TO DISTRIBUTION LIST

13 January 1978

Other Recipients

Mr. Donald Mortel (1)
AF Aero Propulsion Lab.
ATTN: AFAPL-POE-1
Wright-Patterson AFB, Ohio 45433

Mr. Richard E. Oderwald (1)
Department of the Navy
Hqs., US Marine Corps
Code LMC 4
Washington, DC 20380

Commander (1)
Harry Diamond Laboratories
Attn: DELHD-RDD (Mr. A. Benderly
2800 Powder Mill Road
Adelphi, MD 20783

Distribution List - Continued

Electrochimica (1)
2485 Charleston Road
Mountain View, CA 94040
ATTN: Dr. Eisenberg

Dr. Hugh Barger (1)
P.O. Box 2232
Davidson, NC 28036

Energy Storage & Conversion Dept. (1)
TRW Systems
One Space Park
Redondo Beach, CA 90278
ATTN: Dr. H. P. Silverman

Sanders Associates, Inc. (1)
24 Simon Street
Mail Stop NSI-2208
Nashua, NH 03060
ATTN: J. Marshall

Power Conversion, Inc. (1)
70 MacQuesten Pkwy
Mount Vernon, NY 10550
ATTN: Stuart Chodosh

Dr. D. Pouli (1)
Protfolio Manager
Hooker Chemicals & Plastics Corp.
M.P.O. Box 8
Niagara Falls, NY 14302

Dr. Leonard Nanis (1)
G207
S.R.I.
Menlo Park, CA 94025

Dr. J. J. Auborn, RM 1A-317 (1)
Bell Laboratories
600 Mountain Avenue
Murray Hill, NJ 07974

Stonehart Associates, Inc. (1)
34 Five Fields Road
Madison, CT 06443
ATTN: Mr. Thomas Reddy

Jet Propulsion Laboratory (1)
4800 Oak Grove Drive
Pasadena, California 91103
ATTN: Mr. Harvey Frank
Mail Stop 198-220

Mr. J. R. Moden (1)
Energy Conversion Branch Code 3642
Naval Underwater Systems Center
Newport Laboratory
Newport, RI 02840

NASA Lewis Research Center (1)
Mail Stop 6-1
21000 Brookpark Road
Cleveland, OH 44135
ATTN: Dr. Stuart Fordyce

Mr. Joe McCartney (1)
Naval Undersea Center
Code 608
San Diego, CA 92132

EIC, Inc. (1)
ATTN: S. B. Brummer
Newton, MA 02158

Altus Corp. (1)
440 Page Mill Road
Palo Alto, CA 94306
ATTN: Douglas Glader

J. Bene (1)
MS 488
NASA Langley Research Center
Hampton, VA 23665

Mr. Eddie T. Seo (1)
Research and Development Div.
The Gates Rubber Co.
999 S. Broadway
Denver, CO 80217

Mr. Sidney Gross (1)
Mail Stock 8C-62
Boeing Aerospace Company
P. O. Box 3999
Seattle, WA 98124

Honeywell Technology Center (1)
ATTN: Dr. H. V. Venkatesetty
10701 Lyndale Avenue South
Bloomington, MN 55420

Mr. Aiji Uchiyama (1)
Jet Propulsion Laboratory - M.S. 198-220
4800 Oak Grove Drive
Pasadena, CA 91103

Distribution List Continued

Mr. Frank Bis (1)
Naval Surface Weapons Center
White Oak Laboratory, Code R-33
Silver Spring, MD 20910

Transportation Systems Center (1)
Kendall Square
Cambridge, MA 02142
ATTN: Dr. Norman Rosenberg

GTE Laboratories, Inc. (1)
40 Sylvan Road
Waltham, MA 02154

Foote Mineral Company (1)
Route 100
Exton, PA 19341
ATTN: Dr. H. Grady

Honeywell, Inc. (1)
104 Rock Road
Horsham, PA 19044
ATTN: C. Richard Walk

Sanders Associates, Inc. (1)
Sonobuoy Division
95 Canal Street
Nashua, N.H. 03060
ATTN: Mr. David Dwyer

Eagle-Picher Industries, Inc. (1)
Electronics Division
ATTN: Mr. Robert L. Higgins
P.O. Box 47
Joplin, Missouri 64801

Yardney Electric Company (1)
82 Mechanic Street
Pawcatuck, CT 06379
ATTN: Technical Library

Exxon Research and Engineering Co. (1)
Corporate Research Laboratory
Linden, N.J. 07036
ATTN: Dr. R. Hamlen

Argonne National Laboratories (1)
9700 South Cass
Argonne, IL 60439
ATTN: Dr. E. C. Gay

GTE Sylvania, Inc. (1)
77 A Street
Needham Heights, MA 02194
ATTN: Mr. Richard Pabst

General Motors Corp. (1)
Research Laboratories
General Motors Technical Center
12 Mile and Mounds Roads
Warren, MI 48090
ATTN: Dr. J. L. Hartman

Union Carbide Corporation (1)
Parma Research Center
P. O. Box 6116
Cleveland, OH 44101

P. R. Mallory & Co. Inc. (1)
S. Broadway
Tarrytown, N.Y. 10591
ATTN: J. Dalfonso

North American Rockwell Corp. (1)
Atomics International Division
Box 309
Canoga Park, CA 91304
ATTN: Dr. L. Heredy

General Electric Research & (1)
Development Center
P. O. Box 8
Schenectady, N.Y. 12301
ATTN: Dr. Stefan Mitoff

University of California (1)
Department of Science & Research
Santa Barbara, CA 93100
ATTN: Dr. J. Kennedy

The Electric Storage BatteryCo. (1)
Carl F. Norburg Research Center
19 W. College Avenue
Yardley, PA 19067
ATTN: Dr. A. Salkind

Gulton Industries, Inc. (1)
Metuchen, N.J. 08840
ATTN : Mr. S. Charlip